Bibliografia

1 Garcia, G. N. **Direct brain-computer communication through scalp recorded EEG signals**. *Doctor's thesis, Department of Electricity, Ecole Polytechnique Fédérale de Lausanne, Lausanne.* 2004.

2 Millan, J. d. R. **Brain-Computer Interfaces, Handbook of Brain Theory and Neural Networks**. *Cambridge, MA, The MIT Press.* 2, 2002.

3 Norris, F. H. **Amyotrophic lateral sclerosis: The clinical disorder**. *In R. A. Smith (Ed), Handbook ofAmyottrophic Lateral Sclerosis.* (pp.3–38). New York: Marcel Dekker., 1992.

4 Birbaumer, N. **Slow cortical potentials: Plasticity, operant control,and behavioral effects**. *The Neuroscientist, 5, 74–78.* 1999.

5 Birbaumer N, Elbert T, Canavan AGM, Rockstroh B. **Slow cortical potentials of the cerebral cortex and behavior**. Physiol Rev 70:1–41. 1990.

6 Kubler, A., Kotchoubey, B., Kaiser, J., Wolpaw, J., & Birbaumer, N. Brain-computer communication: Unlocking the locked-in. ***Psychological Bulletin**, 127, 358–375.* 2001.

7 Birbaumer, N., Hinterberger, T., Kubler, A., & Neumann, N. The thought-translation-device (TTD): Neurobehavioral mechanisms and clinical outcome. **IEEE Transactions on Neural Systems and Rehabilitation Engineering**, *11, 120–123.* 2003.

8 Wolpaw, J. R., Birbaumer, N., McFarland, D., Pfurtscheller, G., & Vaughan, T. Brain-computer interfaces for communication and control. **Clinical Neurophysiology**, *113, 767–791.* 2002.

9 Wolpaw, J. R.,&McFarland, D. J. Control of a two-dimensional movement signal by a noninvasive brain–computer interface in humans. **Proceedings of the National Academy of Sciences**, *USA, 101, 17849–17854.* 2004.

10 Schalk, McFarland, Hinterberger,. BCI2000. *http://www.bciresearch.org/.* [Online] 2004.

11 Birbaumer, N. Breaking the silence: Brain–computer interfaces (BCI) for communication and motor control. **Psychophysiology**, *43* . 2005.

12 Kennedy, P. R., Kirby, M. T., Moore, M. M., King, B., & Mallory, A. Computer control using human intracortical local field potentials. **IEEE Transactions on Neural Systems and Rehabilitation Engineering***,12, 339–344.* 2004.

13 Brunner, C., Graimann, B., Huggins, J. E., Levine, S. P., & Pfurtscheller. Phase relationships between different subdural electrode recordings in man. **Neuroscience Letters***, 375, 69–74.* 2005.

14 Carmena, J. M., Lebedev, M. A., Crist, R. E., O'Doherty, J. E., Santucci, D. M., Dimitrov, D. F., et al. Learning to control a brain-machine interface for reaching and grasping by primates. **PLoS Biology***, 1, E42.* 2003.

15 Garcia, G. N. **Direct Brain-Computer Communication**. *Doctor`s thesis.* Lausanne : s.n., 2004.

16 Machado, Angelo. **Neuroanatomia Funcional**. s.l. : Atheneu, 1993.

17 http://www.jcda.ca/article/a25. *JCDA.CA.* [Online] [Citado em: 23 de Agosto de 2010.]

18 B. Obermaier, G. Müller, G. Pfurtscheller. **Virtual Keyboard controlled by spontaneous EEG activity**. 2001.

19 Mourino, J. del R. Millán and J. Asynchronous BCI and local neural classifiers: an overview of the adaptive brain interface project. **IEEE Transactions on Neural Systems and Rehabilitation Engineering**. pp. 159–161, 2003, Vol. 11, 2.

20 Pfurtscheller, G. Graz-bci: State of the Art and Clinical Applications. **IEEE Transactions on Neural Systems and Rehabilitation Engineering**. pp.177–180, 2003, Vol. 11, 2.

21 B. Rebsamen, E. Burdet, C. Guan, C. L. Teo, Q. Zeng, M. Ang, C. Laugier. Controlling a wheelchair using a BCI with low information transfer rate. **IEEE International Conference on Rehabilitation Robotics (ICORR)**. 2007, Vols. pp. 1003-1008.

22 F. Galán, M. Nuttin, E. Lew, P. W. Ferrez, G. Vanacker, J. Philips and J. del R. Millán. A Brain-Actuated Wheelchair: Asynchronous and Non-Invasive Brain-Computer Interfaces for Continuous Control of Robots. **Clinical Neurophysiology**. pp. 2159–2169, 2008, Vol. 119.

23 I. Iturrate, J. Antelis, A. Kübler, J. Minguez. A noninvasive brain-actuated wheelchair based on a P300 neurophysiological protocol and automated navigation. **IEEE Transactions on Robotics**. pp. 1–14, 2009, Vol. 99.

24 J. d. R. Millán, F. Renkens, J. Mouriño, W. Gerstner. Noninvasive Brain-Actuated Control of a Mobile Robot by Human EEG. **IEEE Transactions on Biomedical Engineering**. pp 1026-1033, 2004, Vol. 51, 6.

25 E. R. Kandel, J. H. Schwartz, and T. M. Jessell. **Principles of Neural Science**. 1991, 3.

26 Neuro Development Center. *http://www.neurodevelopmentcenter.com.* [Online] [Citado em: 30 de Julho de 2010.]

27 10-20 System of Electrode Placement. [Online] [Citado em: 07 de Julho de 2010.] http://faculty.washington.edu/chudler/1020.html.

28 W. W. Orrison Jr., J. D. Lewine, J. A. Sanders, and M. F. Hartshorne. **Functions Brain Imaging**. St Louis : Mosby-Year Book, Inc, 1995.

29 *http://fc.units.it/ppb/neurobiol/neuroscienze%20per%20tutti/1020.html.* [Online] [Citado em: 23 de Agosto de 2010.]

30 Skinner, B. F. **The Behavior of Organizms**, NewYork: Appleton, 1938.

31 Vaughan, T. M., et al. Brain-Computer Interface Technology: A Review of the Second International Meeting, **IEEE Transactions on Neural Systems and Rehabilitation Engineering**, 11(2):94–109, June 2003.

32 Miller, N. Learning of visceral and glandular responses. **Science**. 163, 434–445, 1969.

33 Skinner, F. **Science and Human Behavior**. NewYork: Macmillan, 1953.

34 Kamiya, J. **Biofeedback and self-control: An Aldine reader**. *Chicago: Aldine.* 1971.

35 Birbaumer, N. Operant enhancement of EEG-theta activity: Aspiration and reality. *In J. Beatty & H. Legewie (Eds.),* **Biofeedback and Behavior** *(pp. 135–146). New York: Plenum Press.* 1977.

36 Sterman, M. B. EEG biofeedback: Physiological behavior modification. **Neuroscience and Biobehavioral Reviews**. 5, 1981, Vols. , 405–412.

37 Pfurtscheller, G., Neuper, C., & Birbaumer, N. Human brain–computer interface (BCI). *In A. Riehle & E. Vaadia (Eds.),* **Motor cortex in voluntary movements. A distributed system for distributed functions** *(pp. 367–401). Boca Raton, FL: CRC Press.* 2005.

38 Jeannerod, M. J. Mental imagery in the motor context. **Neuropsychologia**. 33(11):1419–1432, 1995.

39 Nikolaev, A. R. e Anokhin, A. P. Eeg frequency ranges during perception and mental Rotation of two and three dimentional objects. **Neuroscience and Behavioral Physiology**, *6(28):670–677, 1998.*

40 Galin, D. e Ornstein, R. F. **Human Behavior and Brain Function**,. *chapter Hemispheric Specialization and the Duality of Consciousness, pp. 3–23, Thomas Books, 1975.*

41 Rotenberg, V. S. e Arshavsky, V. V. Right and left brain hemispheres activation in the representatives of two different cultures. **Homeostasis in Health & Disease***, 38(2):49–57, 1997.*

42 Sutter, E.E. The brain response interface: communication through visually-induced. **Journal of Microcomputer Applications**. pp. 31—45, 1992.

43 Bragdon, R.M. Chapman and H.R. Evoked responses to numerical and nonnumerical. **Nature**. pp. 1155 - 1157, 1964, Vol. 203.

44 John, S. Sutton and M. Braren and J. Zublin and E. Evoked potential correlates of. **Science**. pp. 1187 - 1188, 1965, Vol. 150.

45 Donchin, L.A. Farwell and E. Talking off the top of the head: toward a mental prosthesis utilizing event-related brain potentials. **Electroenceph. Clin. Neurophysiol**. pp. 510—523, 1988.

46 Schwartz, Andrew B. **Cortical Neural Prosthetics**. Pittsburgh, Pennsylvania : Departments of Neurobiology and Bioengineering, University of Pittsburgh, 2004.

47 Meel Velliste, Sagi Perel, M. Chance Spalding, Andrew S. Whitford and Andrew B. Schwartz. Cortical control of a prosthetic arm for self-feeding. **Nature**. 2008.

48 Machado, Saulo Jesiel Siqueira. **Desenvolvimento de um sistema de captura e processamento de sinais eletroencefalográficos quantitativo não-invasivo**. *Universidade Federal de Uberlândia.*

49 Van de Velde, M., Van Erp, G. e Cluitmans, P. J. M. Detection of muscle artifact in the normal human awake EEG. **Electroencephalography and Clinical Neurophysiology**. 107(2):149–158, April1998.

50 TORELLO, M. Topographic mapping of EEG and evoked potentials in psychiatry:Delusions, illusions, and realities. **Brain Topography**.

51 HAYKIN S. 1994. ***Neural Networks: A Comprehensive Foundation*****. Macmillan**, New York, NY.

52 Dan Griffiths, Nelo, Jim Peters, Andreas Robinson, Jack Spaar. OpenEEG. *http://openeeg.sourceforge.net/doc/index.html.* [Online] [Citado em: 17 de 07 de 2010.]

53 Benning, M., et al. **The Experimental Portable EEG/EMG Amplifier**. *ELEC 499A Report, University of Victoria, Faculty of Engineering.* 2003.

54 Joseph J. Carr, John M. Brown. **Introduction to Biomedical Equipment Technology**. 4th edition, 2001 isbn 0-13-010492-2.

55 http://focus.ti.com/docs/prod/folders/print/ina114.html. [Online] 26 de Julho de 2010.

56 http://sine.ni.com/nips/cds/view/p/lang/en/nid/201987. [Online] 26 de Julho de 2010.

57 Babiloni F, Cincotti F, Carducci F, Rossini PM, Babiloni C. Spatial enhancement of EEG data by surface Laplacian estimation: the use of magnetic resonance imaging-based head models. **Clin Neurophysiol**. 112:724–7, 2001.

58 PL., Nunez. Toward a quantitative description of large-scale neocortical dynamic function and EEG. **Behav Brain Sci**. 23:371–437, 2000.

59 PL., Nunez. Electric fields of the brain. **New York: Oxford University Press**. 1981.

60 B., Hjorth. An on-line transformation of EEG scalp potentials into orthogonal source derivations. **Electroenceph Clin Neurophysiol**. 526–30, 1975, Vol. 39.

61 C. Tandonnet, B.Burle, T.Hasbroucq, F.Vidal. Spatial enhancement of EEG traces by surface Laplacian estimation: comparison between local and global methods. **Clinical Neurophysiology**. pp. 18-24, 2005, Vol. 116, 1.

62 Akay, M. Wavelets applications in medicine. **Spectrum**. pp. 50-57, 1997.

63 Sergio Fugivara, Alison de O. Moraes, José C. J. de Almeida. **Aplicação da transformada de wavelets para compressão de dados de telemetria**. *CTA – Centro Técnico Aeroespacial.*

64 A.O.G. Barbosa, D.R. Achanccaray, M. Vellasco, M.A. Meggiolaro, R. Tanscheit. Mental Tasks Classification for a Noninvasive BCI Application. **19th International Conference on Artificial Neural Networks, ICANN'09, Limassol, Cyprus**. 2009.

65 D.R. Achanccaray, M.A. Meggiolaro. Brain Computer Interface Based on Electroencephalographic Signal Processing. **XVI IEEE International Congress of Electrical, Electronic and Systems Engineering** - *INTERCON 2009, Arequipa, Peru, 2009.*

66 Alexandre O. G. Barbosa, David R. Achanccaray, and Marco A. Meggiolaro. Activation of a Mobile Robot through a Brain Computer Interface. *2010* **IEEE International Conference on Robotics and Automation, Anchorage Convention District***, May 3-8, 2010, Anchorage, Alaska, USA.* 2010.

Anexos

I. Circuito esquemático do eletroencefalógrafo.

II. Circuito impresso do eletroencefalógrafo.

III. Circuito esquemático da eletrônica do manipulador.

IV. Circuito impresso da eletrônica do manipulador.

V. Código do microcontrolador da eletrônica do manipulador.

VI. *Datasheet* do amplificador instrumental INA114.

Anexo I

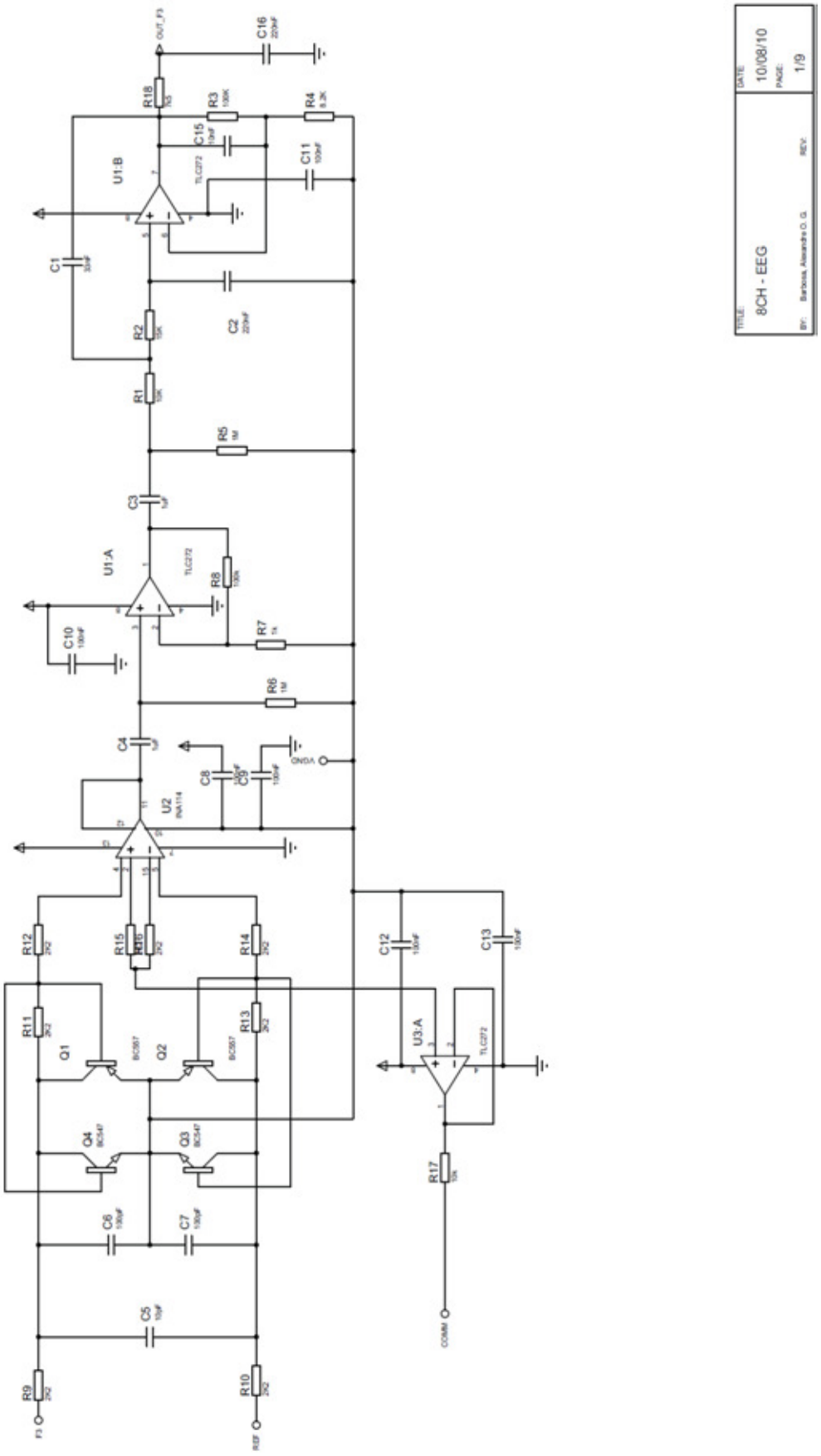

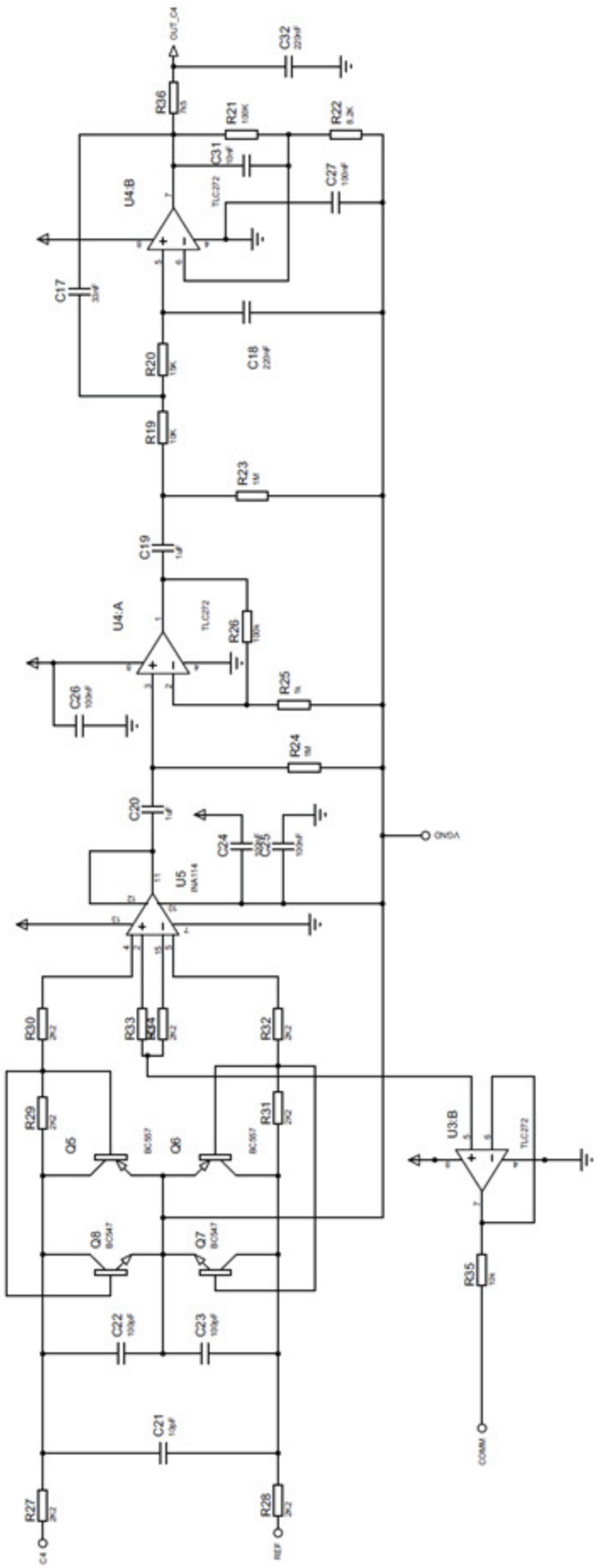

TITLE: 8CH - EEG	DATE: 10/08/10
BY: Barbosa, Alexandre G. G.	REV: PAGE: 2/9

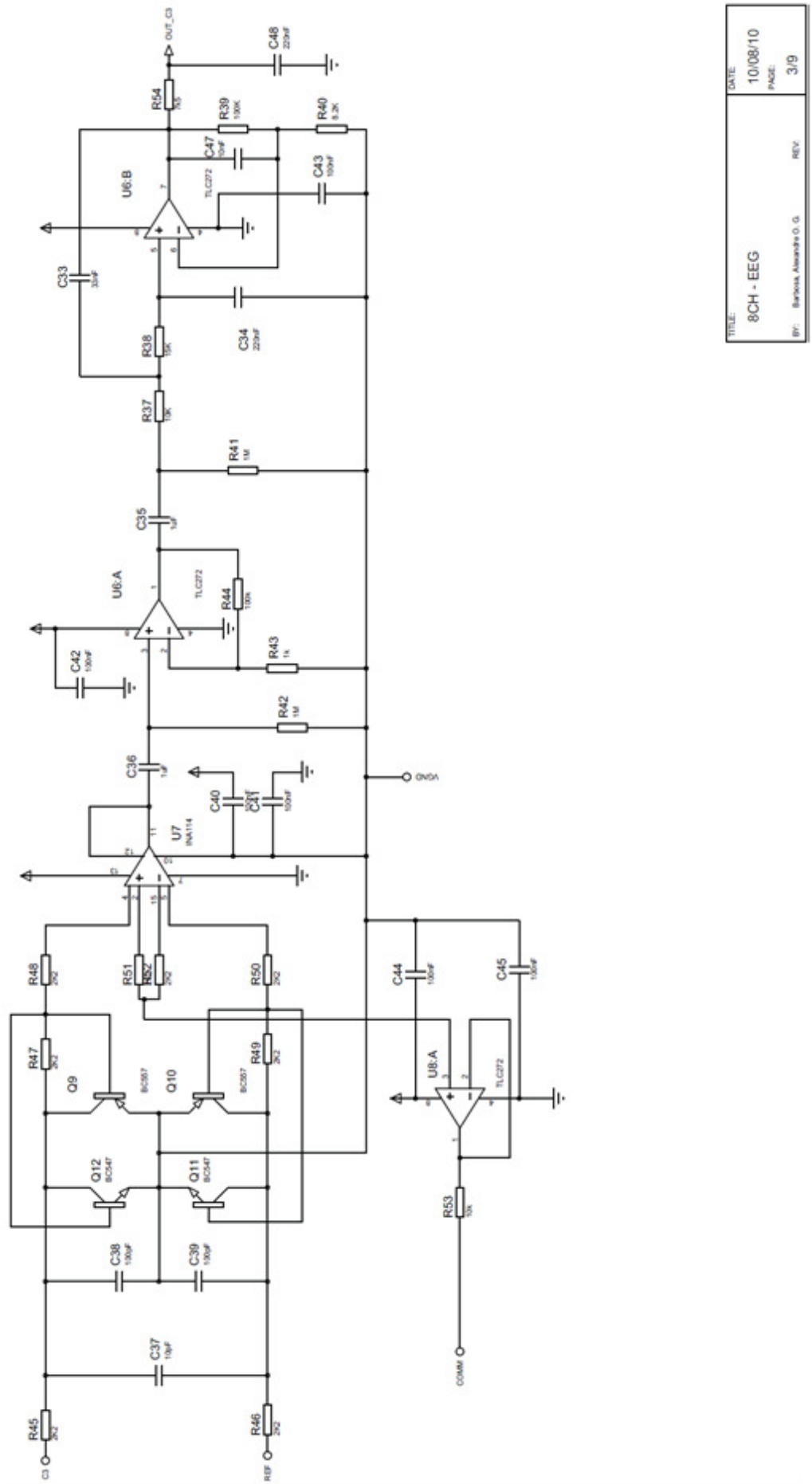

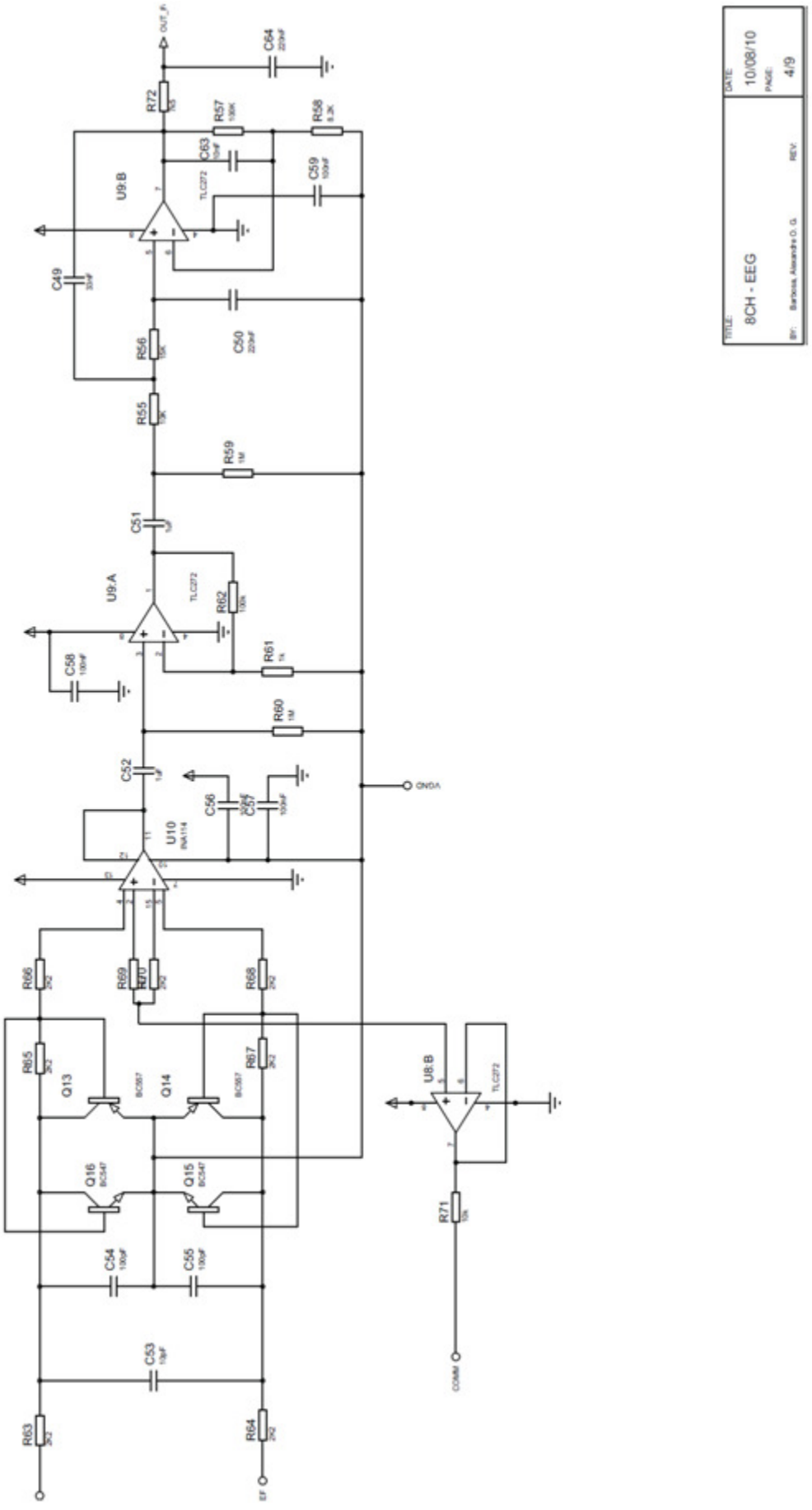

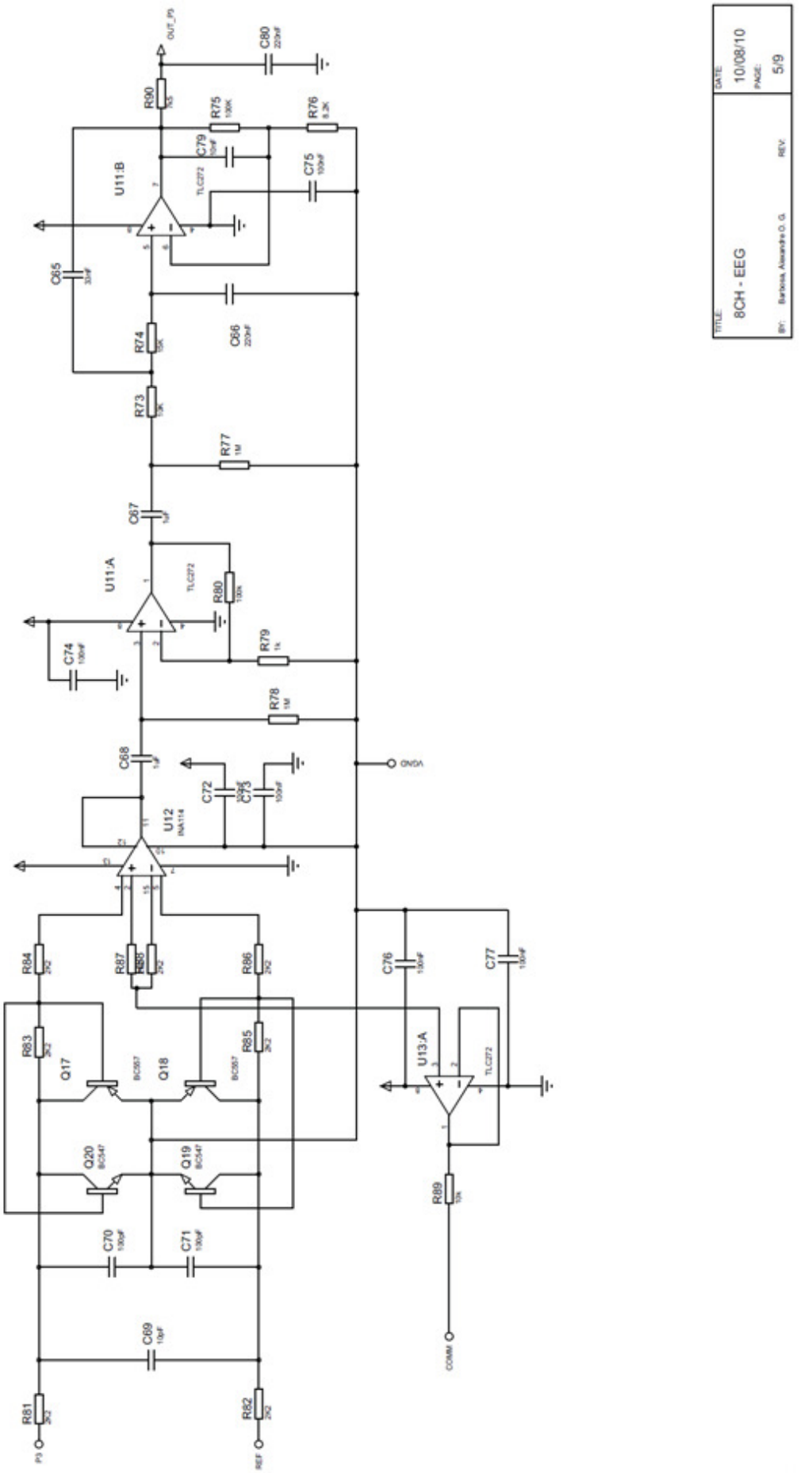

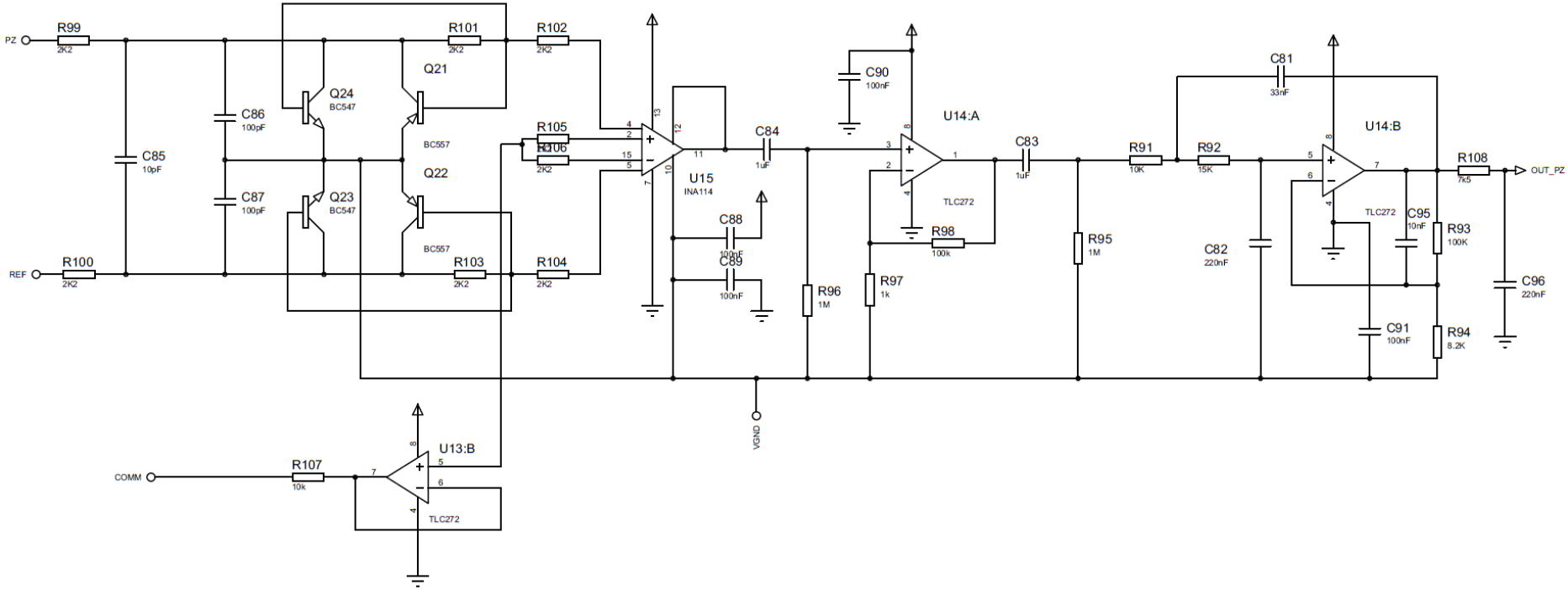

TITLE:	DATE:
8CH - EEG	10/08/10
	PAGE: 6/9
BY: Barbosa, Alexandre O. G.	REV:

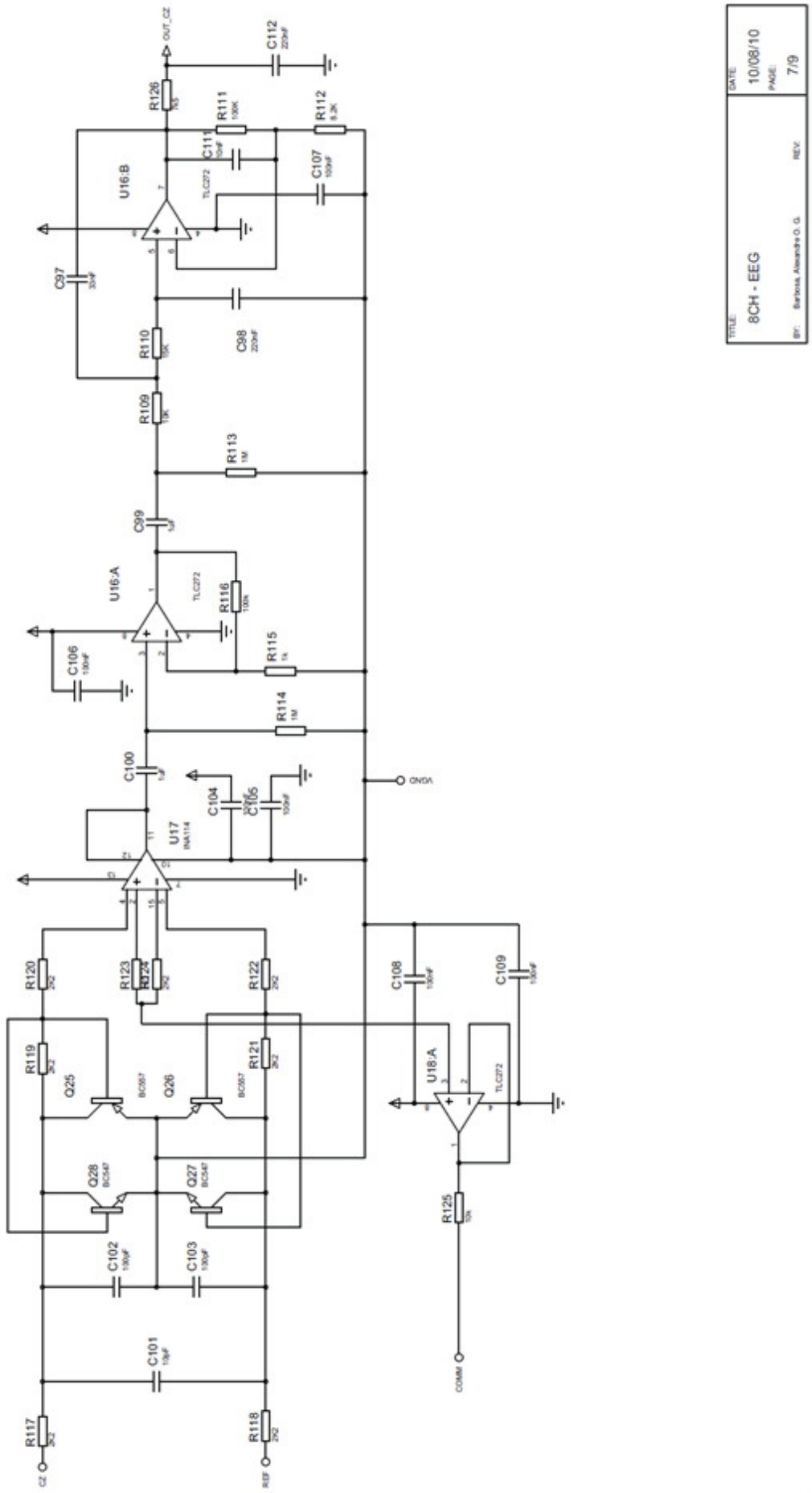

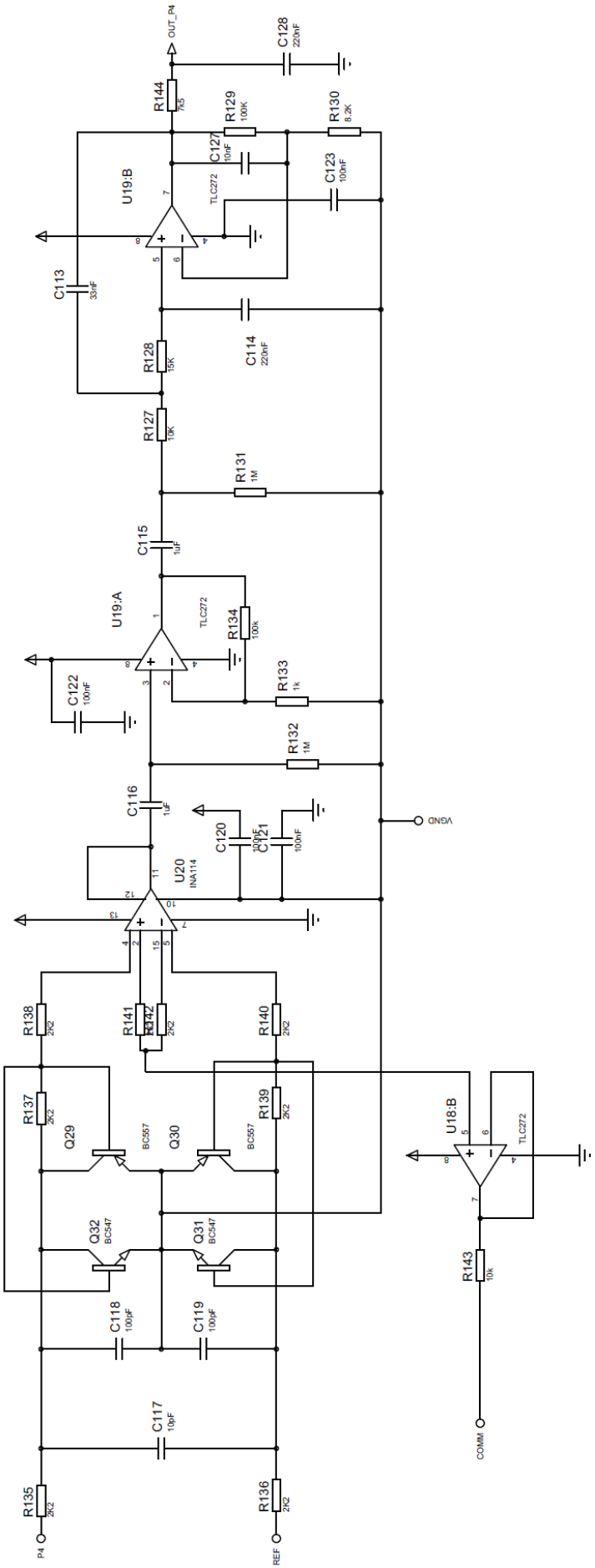

TITLE: 8CH - EEG	DATE: 10/08/10
BY: Barbosa, Alexandre O. G.	REV: PAGE: 8/9

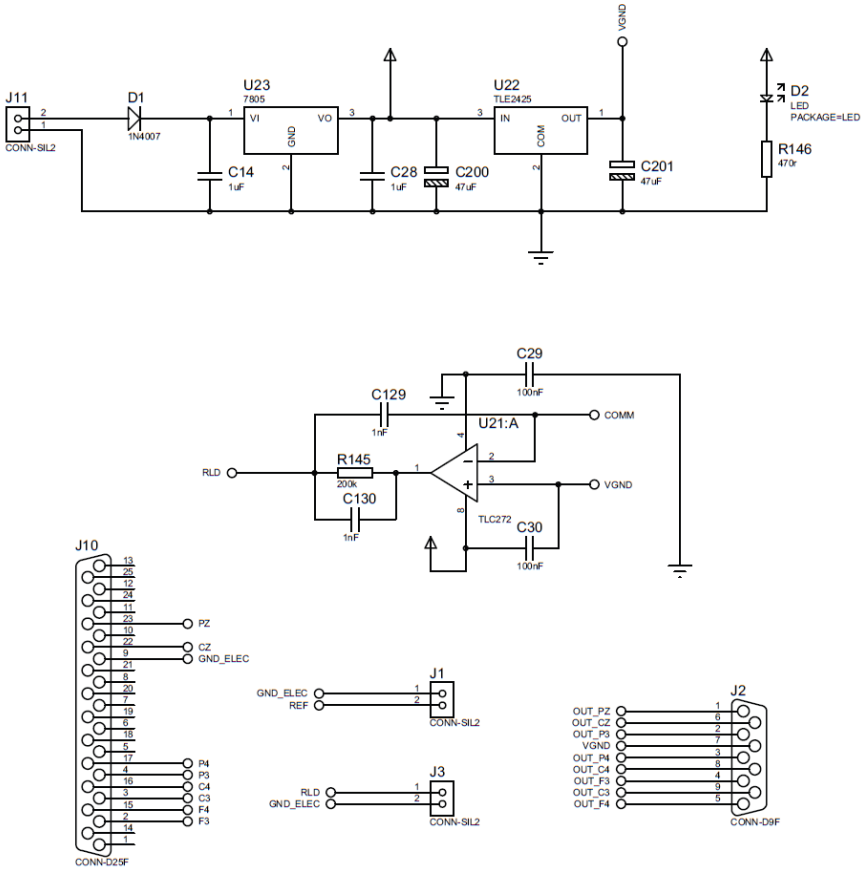

TITLE:	DATE:
8CH - EEG	10/08/10
	PAGE: 9/9
BY: Barbosa, Alexandre O. G. REV:	

Anexo II

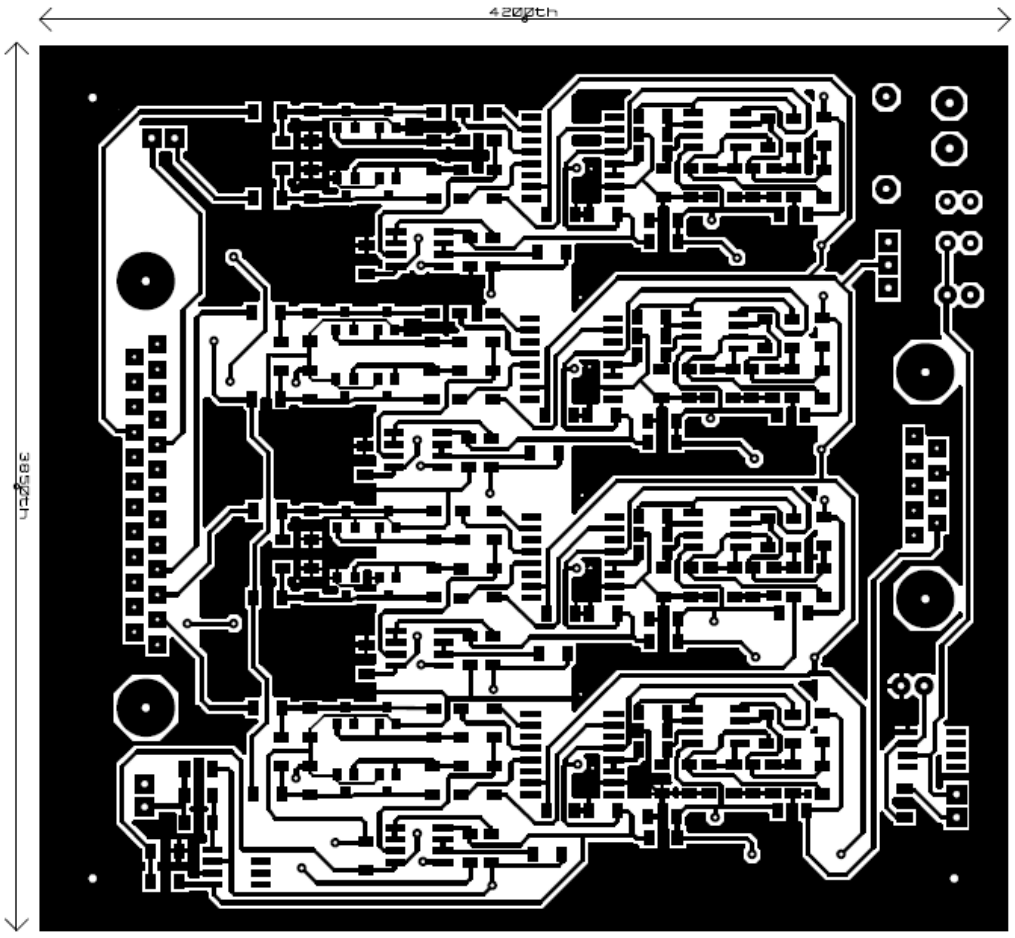

Face Superior

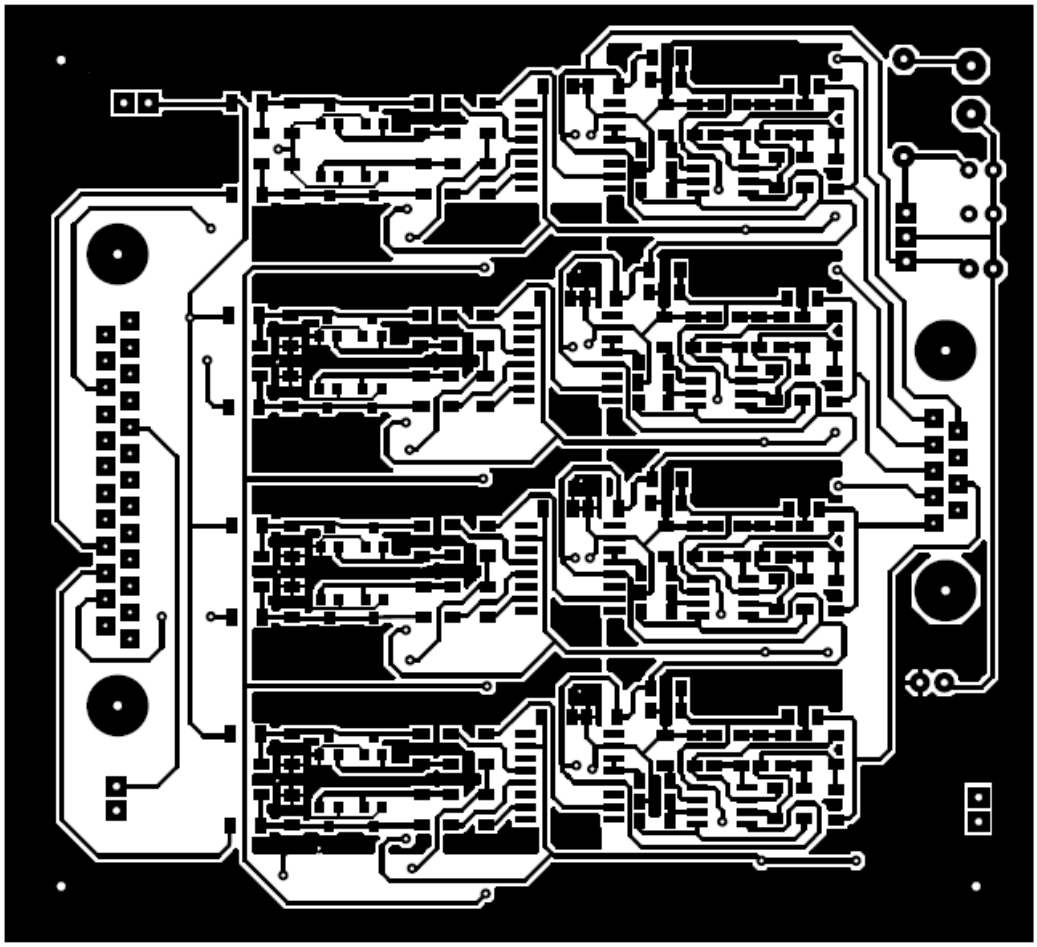

Face inferior

Anexo III

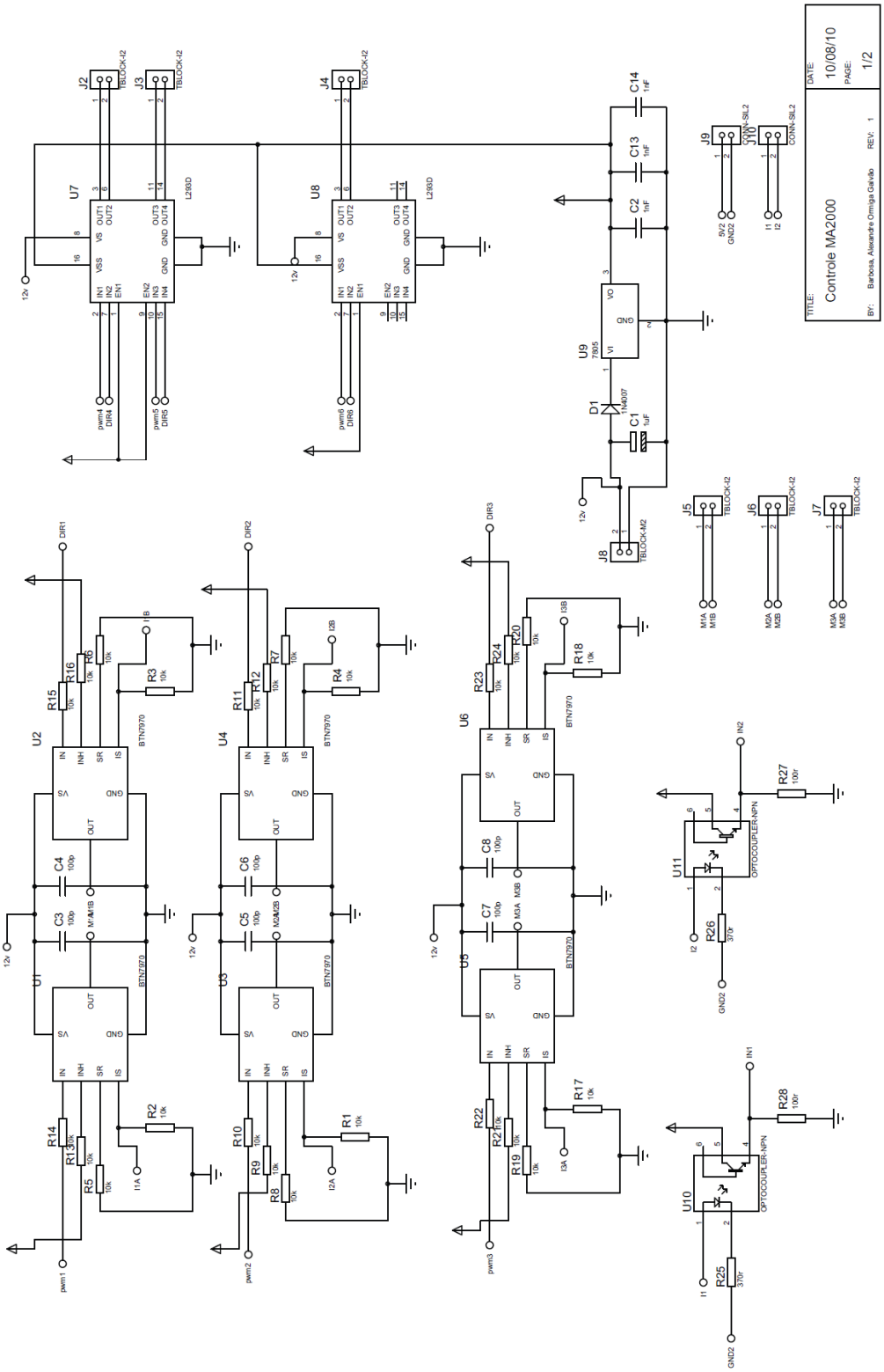

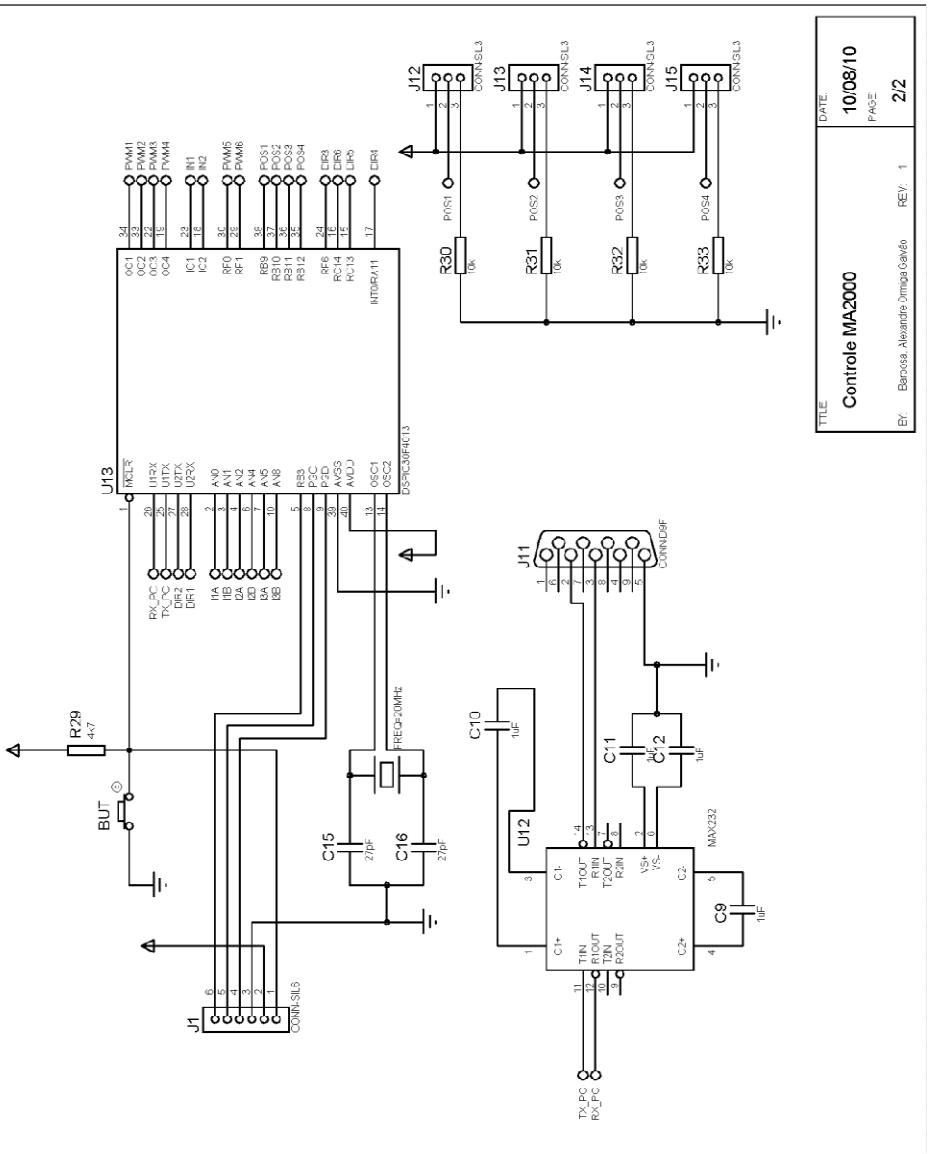

Anexo IV

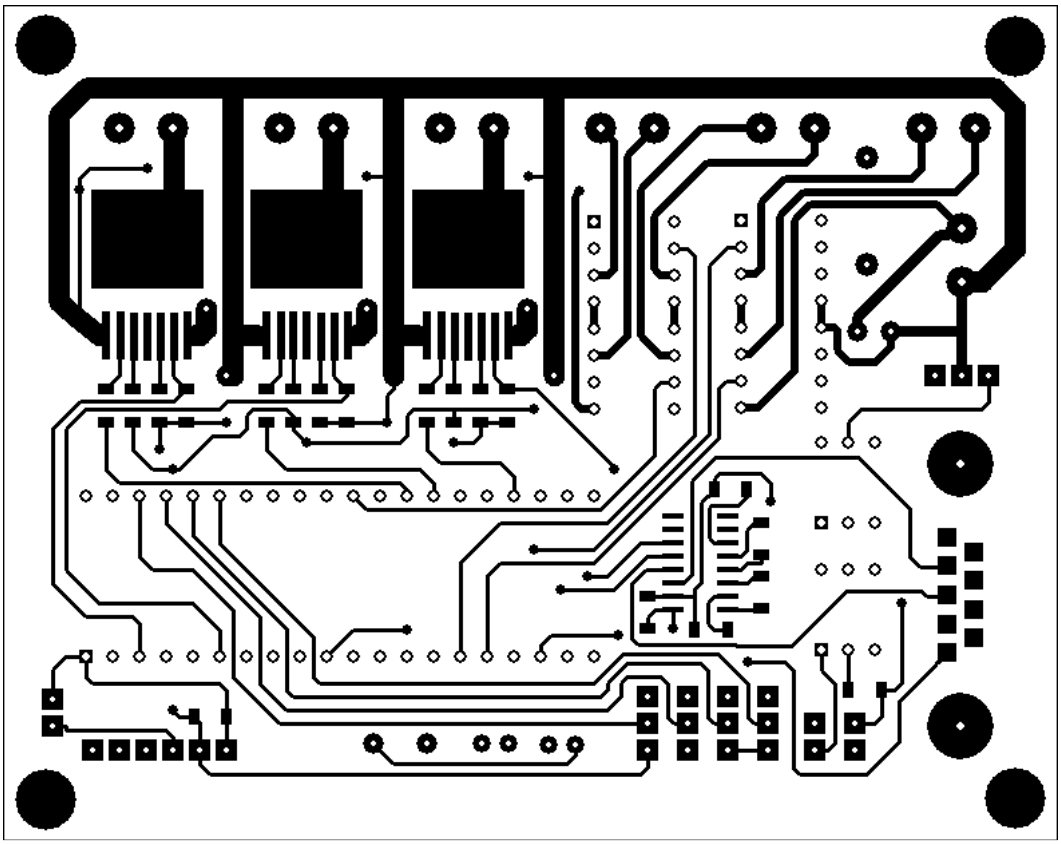

Face superior

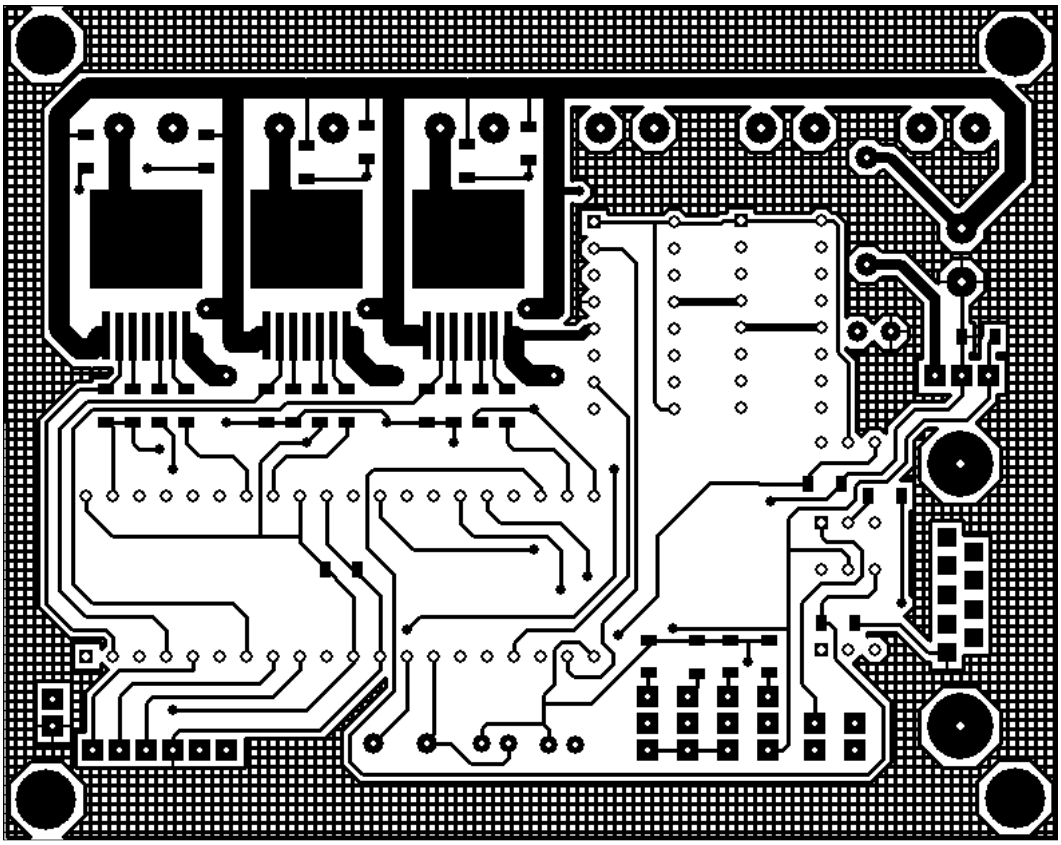

Face inferior

Anexo V

```
#include <30f4013.h>
#DEVICE ADC=16
#FUSES XT_PLL8
#FUSES NOWDT
#use delay(clock=80000000)
#DEFINE DIR_1 PIN_F4
#DEFINE DIR_2 PIN_F5
#DEFINE DIR_3 PIN_F6
#DEFINE DIR_4 PIN_A11
#DEFINE DIR_5 PIN_C13
#DEFINE DIR_6 PIN_C14
#DEFINE I1A 0
#DEFINE I1B 1
#DEFINE I2A 2
#DEFINE I2B 4
#DEFINE I3A 5
#DEFINE I3B 8
#DEFINE POS1 9
#DEFINE POS2 10
#DEFINE POS3 11
#DEFINE POS4 12
#DEFINE eIi_lim 200000
#TYPE SIGNED
#include <stdlib.h>
#include <math.h>
#use rs232(UART1,baud=9600,parity=N,bits=8)

    INT flag, xi, yi, zi, kii, kpi, kdi, kt_m2i, kti;

int16 eIant=0, eiI=0;

float q1=0, q2=0, q3=0, sum,sum2,p1_des, p2_des, p3_des, ep=0, epi[3], epd=0, e
pant[3], iki=0.005, ikp=0.1,kp=30.00,ki=0,kd=0,x,y,z,kt_m2,ang2,kt;

//***************************************************************************
// TRATAMENTO DOS DADOS SERIAIS ////////////////////////////////////////////////
//***************************************************************************
#INT_RDA
```

```
void  RDA_isr()
{
  xi = getc () ;
  yi = getc () ;
  zi = getc () ;
  kpi = getc () ;
  kii = getc () ;
  kdi = getc () ;
  kt_m2i = getc () ;
  kti = getc () ;
  flag = 1;
  x = xi;
  y = yi;
  z = zi;
  kp = (FLOAT) kpi / 100.00;
  ki = (FLOAT) kii / 1000.00;
  kd = (FLOAT) kdi / 100.00;
  kt_m2 = (FLOAT) kt_m2i;
  kt = (FLOAT) kti / 100.00;
}

//*****************************************************************************
// LEITURA DAS POSIÇÕES ////////////////////////////////////////////////////////
//*****************************************************************************
float read_pos(INT link)
{
  FLOAT pos;
  set_adc_channel (link);
  delay_us (10);
  pos = read_adc ();
  RETURN pos;
}

//*****************************************************************************
// Cinemática INVERSA //////////////////////////////////////////////////////////
///
//*****************************************************************************
void id()
{
  flag = 0;
```

```
sum = pwr (x, 2) + pwr (y, 2) + pwr (z, 2);
sum2 = pwr (x, 2) + pwr (y, 2);

IF (y == 0)
{
   y = 0.0001;
}

p1_des = atan (x / y) ;
p2_des = atan (z / (sqrt (sum2))) - acos ((sum - 47.00) / (sqrt (sum)  * 46.00));
p3_des = acos ( ( (pwr (x, 2) + pwr (y,2) + pwr (z, 2)) -1105.0)  / 1104.0);
printf ("LINK1 = %f LINK2 = % f LINK3 = % f",p1_des, p2_des, p3_des);
delay_ms (10) ;
putc (13) ;
delay_ms (10) ;
p1_des = ((p1_des * 360 / 2 / 3.1415) * (65536 - 4183) / 360)   +  35200.00;
p2_des = ((p2_des * 360 / 2 / 3.1415) * (65536 - 4183) / 360)   +  32600.00;
p3_des = ((p3_des * 360 / 2 / 3.1415) * (65536 - 4183) / 360)   +  25000;
printf ("LINK1 = %f LINK2 = % f LINK3 = % f",p1_des, p2_des, p3_des);
delay_ms (10) ;
putc (13) ;
delay_ms (10) ;
printf ("kp = %f ki = % f kd = %f", kp, ki, kd);
delay_ms (10) ;
putc (13) ;
delay_ms (10) ;
printf ("Cons. de Torque = %f kt_pos = % f", kt_m2, kt);
delay_ms (10) ;
putc (13) ;
delay_ms (10) ;
printf ("----------------------------------------------") ;
delay_ms (10) ;
putc (13) ;

IF (p3_des > 65536)
{
   p3_des = p3_des - 65536;
}

IF (p2_des > 65536)
```

```
  {
    p2_des = p2_des - 65536;
  }
}

//*****************************************************************************
// CONTROLE DE POSIÇÃO ////////////////////////////////////////////////////////
//*****************************************************************************
float POS_contr(INT16 channel, float p, float p_des)
{
  FLOAT V = 0, ep1 = 0, ep2 = 0;
  ep = p_des - p;

  IF (ep > 34000)
    ep = - (65536 - ep);

  IF (ep < (-34000))
  ep = (65536 + ep);
  epi[channel] = epi[channel] + ep;
  epd = epant[channel] - ep;

  IF (epi[channel] > 100000)
    epi[channel] = 100000;

  IF (epi[channel] < (-100000))
  epi[channel] = - 100000;
  V = ep * kp + epi[channel] * ki + epd * kd;
  epant[channel] = ep;

  IF (V > 10000)
    V = 10000;

  IF (V < - 10000)
    V = - 10000;

  IF ( (ep < 100)&& (ep >  - 100) )
  V = 0;
  RETURN V;
}
```

```
//*****************************************************************************
// TORQUE GRAVIDADE ////////////////////////////////////////////////////////
//*****************************************************************************
float q_grav (FLOAT ang)
{
  FLOAT i_grav;
  ang = ( (ang - 32600.00) / (65536 - 4183)) * 2 * 3.1415;
  i_grav = cos (ang) * ((0.88 * 9.8 * 0.07) + (0.963 * 9.8 * 0.23)) * kt_m2;
  RETURN i_grav;
}

//*****************************************************************************
// ACIONAMENTO DOS MOTORES ////////////////////////////////////////////////////
//*****************************************************************************
void motor(INT link, float power)
{
  INT16 duty = 0;
  INT pin = 0;

  IF (power >= 0)
  {
    duty = (INT16) power;

    SWITCH (link)
    {
      CASE 1:
      output_low (DIR_1) ;
      set_pwm_duty (1, duty) ;
      BREAK;

      CASE 2:
      output_low (DIR_2) ;
      set_pwm_duty (2, duty) ;
      BREAK;

      CASE 3:
      output_low (DIR_3) ;
      set_pwm_duty (3, duty) ;
      BREAK;
    }
```

```
    }

    ELSE
    {
      duty = (INT16) (10000 + power);

      SWITCH (link)
      {
        CASE 1:
        output_high (DIR_1) ;
        set_pwm_duty (1, duty) ;
        BREAK;

        CASE 2:
        output_high (DIR_2) ;
        set_pwm_duty (2, duty) ;
        BREAK;

        CASE 3:
        output_high (DIR_3) ;
        set_pwm_duty (3, duty) ;
        BREAK;
      }
    }
  }

  //*****************************************************************************
  //*****************************************************************************
  ////////////////////////////////// MAIN ////////////////////////////////////////
  //*****************************************************************************
  //*****************************************************************************
  void main()
  {

    INT loop_PID_POS = 0;

    FLOAT q1_POS = 0, q2_POS = 0, q3_POS = 0, q1_grav = 0, q2_grav = 0,
q3_grav
    = 0, q1_cur = 0, IA = 0, IB = 0;
    FLOAT p1 = 0, p2 = 0, p3 = 0;
```

```
setup_timer1 (TMR_INTERNAL|TMR_DIV_BY_8, 30000) ;
setup_timer2 (TMR_INTERNAL|TMR_DIV_BY_64, 10000) ;
setup_adc (ADC_CLOCK_INTERNAL);
setup_adc_ports (ALL_ANALOG);
enable_interrupts (INT_RDA);
enable_interrupts (INTR_GLOBAL);
setup_compare (1, COMPARE_PWM|COMPARE_TIMER2) ;
setup_compare (2, COMPARE_PWM|COMPARE_TIMER2) ;
setup_compare (3, COMPARE_PWM|COMPARE_TIMER2) ;
setup_compare (4, COMPARE_PWM|COMPARE_TIMER2) ;

output_low (DIR_1) ;
output_low (DIR_2) ;
output_low (DIR_3) ;
set_pwm_duty (1, 0) ;
set_pwm_duty (2, 0) ;
set_pwm_duty (3, 0) ;
p3_des = 23530.00;
p2_des = 32600.00;
p1_des = 35200.00;
delay_ms (2000) ;

//************************************************************************
****
// LOOP PRINCIPAL ////////////////////////////////////////////////////////
////
//************************************************************************
****
WHILE (true)
{
  IF (flag == 1)
  {
    id ();
    flag = 0;
  }

  IF (loop_PID_POS == 1)
  {
    p1 = read_pos (POS1) ;
    p2 = read_pos (POS2) ;
```

```
            p3 = read_pos (POS3) ;
            // printf (" % f % f %f\n\r", p1, p2, p3);
            q1_POS = POS_contr (1, p1, p1_des) ;
            q2_POS = POS_contr (2, p2, p2_des) ;
            q3_POS = POS_contr (3, p3, p3_des) ;

            loop_PID_POS = 0;
          }

          motor (1, q1_POS) ;
          motor (2, q2_POS) ;
          motor (3, q3_POS) ;
          loop_PID_POS++;
        }
}
```

Anexo VI

BURR-BROWN®

INA114

Precision INSTRUMENTATION AMPLIFIER

FEATURES

- LOW OFFSET VOLTAGE: 50µV max
- LOW DRIFT: 0.25µV/°C max
- LOW INPUT BIAS CURRENT: 2nA max
- HIGH COMMON-MODE REJECTION: 115dB min
- INPUT OVER-VOLTAGE PROTECTION: ±40V
- WIDE SUPPLY RANGE: ±2.25 to ±18V
- LOW QUIESCENT CURRENT: 3mA max
- 8-PIN PLASTIC AND SOL-16

APPLICATIONS

- BRIDGE AMPLIFIER
- THERMOCOUPLE AMPLIFIER
- RTD SENSOR AMPLIFIER
- MEDICAL INSTRUMENTATION
- DATA ACQUISITION

DESCRIPTION

The INA114 is a low cost, general purpose instrumentation amplifier offering excellent accuracy. Its versatile 3-op amp design and small size make it ideal for a wide range of applications.

A single external resistor sets any gain from 1 to 10,000. Internal input protection can withstand up to ±40V without damage.

The INA114 is laser trimmed for very low offset voltage (50µV), drift (0.25µV/°C) and high common-mode rejection (115dB at G = 1000). It operates with power supplies as low as ±2.25V, allowing use in battery operated and single 5V supply systems. Quiescent current is 3mA maximum.

The INA114 is available in 8-pin plastic and SOL-16 surface-mount packages. Both are specified for the –40°C to +85°C temperature range.

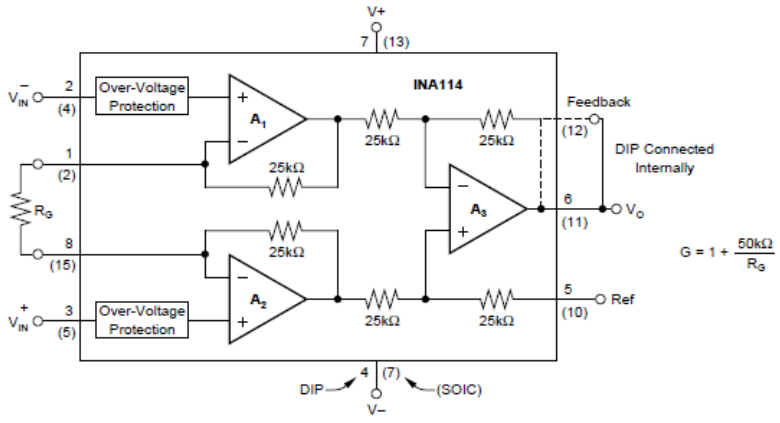

International Airport Industrial Park • Mailing Address: PO Box 11400, Tucson, AZ 85734 • Street Address: 6730 S. Tucson Blvd., Tucson, AZ 85706 • Tel: (520) 746-1111 • Twx: 910-952-1111
Internet: http://www.burr-brown.com/ • FAXLine: (800) 548-6133 (US/Canada Only) • Cable: BBRCORP • Telex: 066-6491 • FAX: (520) 889-1510 • Immediate Product Info: (800) 548-6132

PDS-1142D

Printed in U.S.A. March, 1998

SPECIFICATIONS

ELECTRICAL

At T_A = +25°C, V_S = ±15V, R_L = 2kΩ, unless otherwise noted.

PARAMETER	CONDITIONS	INA114BP, BU MIN	INA114BP, BU TYP	INA114BP, BU MAX	INA114AP, AU MIN	INA114AP, AU TYP	INA114AP, AU MAX	UNITS
INPUT								
Offset Voltage, RTI								
Initial	T_A = +25°C		±10 + 20/G	±50 + 100/G		±25 + 30/G	±125 + 500/G	µV
vs Temperature	T_A = T_{MIN} to T_{MAX}		±0.1 + 0.5/G	±0.25 + 5/G		±0.25 + 5/G	±1 + 10/G	µV/°C
vs Power Supply	V_S = ±2.25V to ±18V		0.5 + 2/G	3 + 10/G		*	*	µV/V
Long-Term Stability			±0.2 + 0.5/G			*		µV/mo
Impedance, Differential			10^{10} || 6			*		Ω || pF
Common-Mode			10^{10} || 6			*		Ω || pF
Input Common-Mode Range		±11	±13.5		*	*		V
Safe Input Voltage				±40			*	V
Common-Mode Rejection	V_{CM} = ±10V, ΔR_S = 1kΩ							
	G = 1	80	96		75	90		dB
	G = 10	96	115		90	106		dB
	G = 100	110	120		106	110		dB
	G = 1000	115	120		106	110		dB
BIAS CURRENT			±0.5	±2		*	±5	nA
vs Temperature			±8			*		pA/°C
OFFSET CURRENT			±0.5	±2		*	±5	nA
vs Temperature			±8			*		pA/°C
NOISE VOLTAGE, RTI	G = 1000, R_S = 0Ω							
f = 10Hz			15			*		nV/√Hz
f = 100Hz			11			*		nV/√Hz
f = 1kHz			11			*		nV/√Hz
f_B = 0.1Hz to 10Hz			0.4			*		µVp-p
Noise Current								
f=10Hz			0.4			*		pA/√Hz
f=1kHz			0.2			*		pA/√Hz
f_B = 0.1Hz to 10Hz			18			*		pAp-p
GAIN								
Gain Equation			1 + (50kΩ/R_G)			*		V/V
Range of Gain		1		10000	*		*	V/V
Gain Error	G = 1		±0.01	±0.05		*	*	%
	G = 10		±0.02	±0.4		*	±0.5	%
	G = 100		±0.05	±0.5		*	±0.7	%
	G = 1000		±0.5	±1		*	±2	%
Gain vs Temperature	G = 1		±2	±10		*	±10	ppm/°C
50kΩ Resistance[1]			±25	±100		*	*	ppm/°C
Nonlinearity	G = 1		±0.0001	±0.001		*	±0.002	% of FSR
	G = 10		±0.0005	±0.002		*	±0.004	% of FSR
	G = 100		±0.0005	±0.002		*	±0.004	% of FSR
	G = 1000		±0.002	±0.01		*	±0.02	% of FSR
OUTPUT								
Voltage	I_O = 5mA, T_{MIN} to T_{MAX}	±13.5	±13.7		*	*		V
	V_S = ±11.4V, R_L = 2kΩ	±10	±10.5		*	*		V
	V_S = ±2.25V, R_L = 2kΩ	±1	±1.5		*	*		V
Load Capacitance Stability			1000			*		pF
Short Circuit Current			+20/–15			*		mA
FREQUENCY RESPONSE								
Bandwidth, –3dB	G = 1		1			*		MHz
	G = 10		100			*		kHz
	G = 100		10			*		kHz
	G = 1000		1			*		kHz
Slew Rate	V_O = ±10V, G = 10	0.3	0.6		*	*		V/µs
Settling Time, 0.01%	G = 1		18			*		µs
	G = 10		20			*		µs
	G = 100		120			*		µs
	G = 1000		1100			*		µs
Overload Recovery	50% Overdrive		20			*		µs
POWER SUPPLY								
Voltage Range		±2.25	±15	±18	*	*	*	V
Current	V_{IN} = 0V		±2.2	±3		*	*	mA
TEMPERATURE RANGE								
Specification		–40		85	*		*	°C
Operating		–40		125	*		*	°C
θ_{JA}			80			*		°C/W

* Specification same as INA114BP/BU.

NOTE: (1) Temperature coefficient of the "50kΩ" term in the gain equation.

PIN CONFIGURATIONS

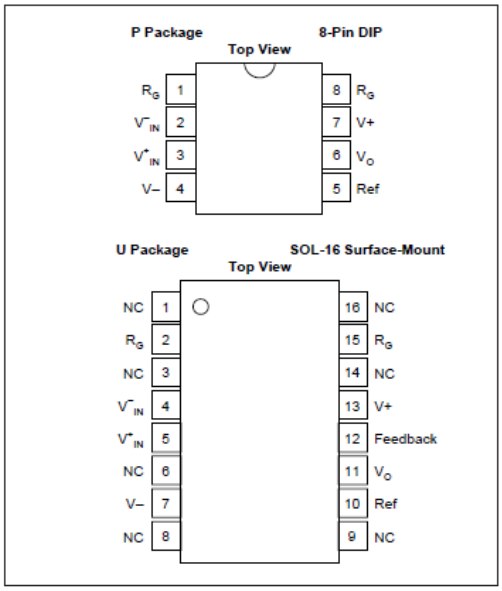

ABSOLUTE MAXIMUM RATINGS(1)

Supply Voltage	±18V
Input Voltage Range	±40V
Output Short-Circuit (to ground)	Continuous
Operating Temperature	–40°C to +125°C
Storage Temperature	–40°C to +125°C
Junction Temperature	+150°C
Lead Temperature (soldering, 10s)	+300°C

NOTE: (1) Stresses above these ratings may cause permanent damage.

ELECTROSTATIC DISCHARGE SENSITIVITY

This integrated circuit can be damaged by ESD. Burr-Brown recommends that all integrated circuits be handled with appropriate precautions. Failure to observe proper handling and installation procedures can cause damage.

ESD damage can range from subtle performance degradation to complete device failure. Precision integrated circuits may be more susceptible to damage because very small parametric changes could cause the device not to meet its published specifications.

PACKAGE/ORDERING INFORMATION

PRODUCT	PACKAGE	PACKAGE DRAWING NUMBER(1)	TEMPERATURE RANGE
INA114AP	8-Pin Plastic DIP	006	–40°C to +85°C
INA114BP	8-Pin Plastic DIP	006	–40°C to +85°C
INA114AU	SOL-16 Surface-Mount	211	–40°C to +85°C
INA114BU	SOL-16 Surface-Mount	211	–40°C to +85°C

NOTE: (1) For detailed drawing and dimension table, please see end of data sheet, or Appendix C of Burr-Brown IC Data Book.

TYPICAL PERFORMANCE CURVES

At T_A = +25°C, V_S = ±15V, unless otherwise noted.

GAIN vs FREQUENCY

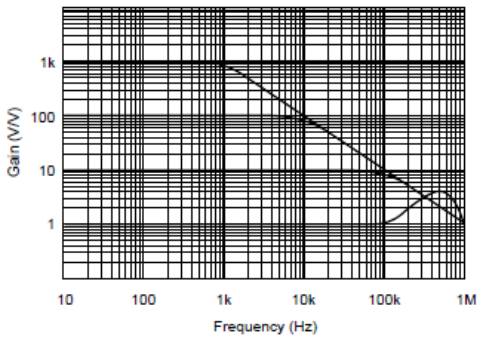

COMMON-MODE REJECTION vs FREQUENCY

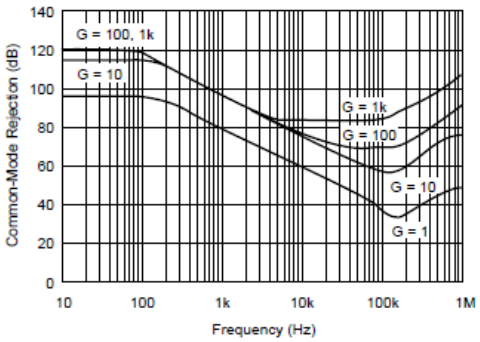

INPUT COMMON-MODE VOLTAGE RANGE vs OUTPUT VOLTAGE

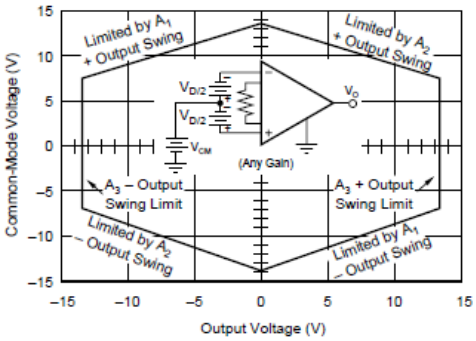

POSITIVE POWER SUPPLY REJECTION vs FREQUENCY

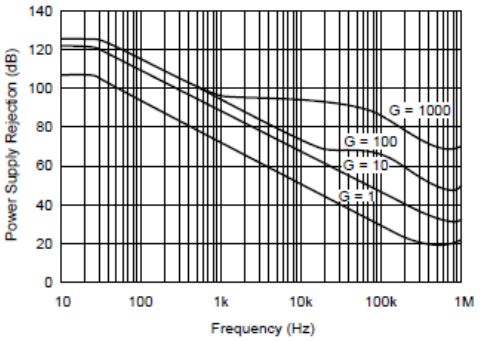

NEGATIVE POWER SUPPLY REJECTION vs FREQUENCY

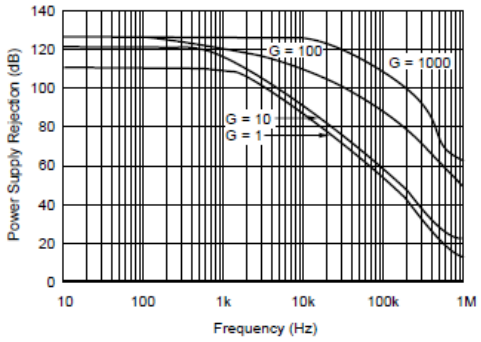

INPUT-REFERRED NOISE VOLTAGE vs FREQUENCY

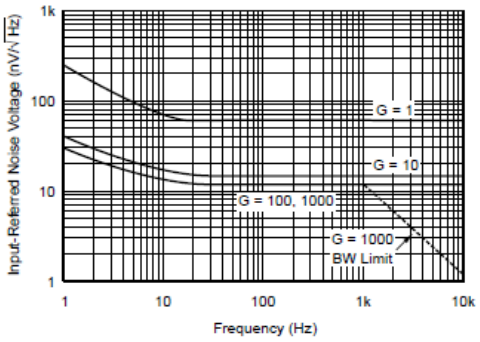

TYPICAL PERFORMANCE CURVES (CONT)

At T_A = +25°C, V_S = ±15V, unless otherwise noted.

SETTLING TIME vs GAIN

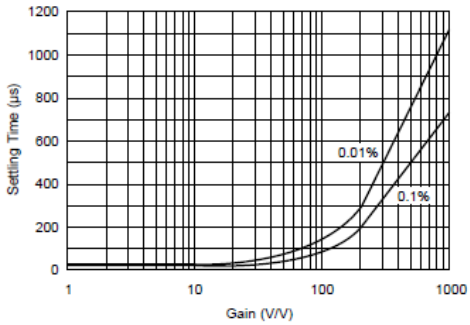

OFFSET VOLTAGE WARM-UP vs TIME

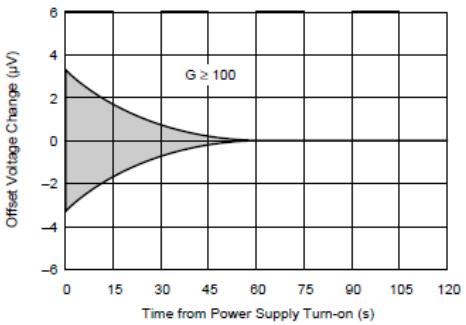

INPUT BIAS AND INPUT OFFSET CURRENT vs TEMPERATURE

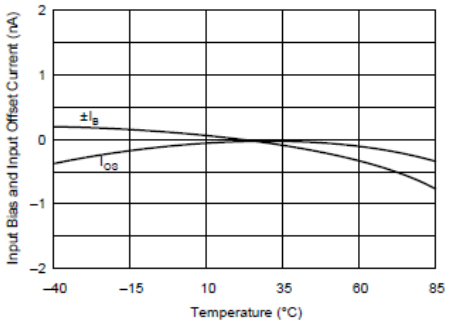

INPUT BIAS CURRENT vs DIFFERENTIAL INPUT VOLTAGE

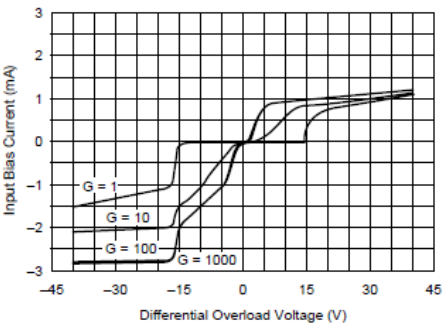

INPUT BIAS CURRENT vs COMMON-MODE INPUT VOLTAGE

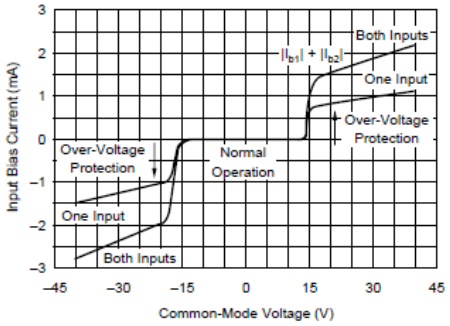

MAXIMUM OUTPUT SWING vs FREQUENCY

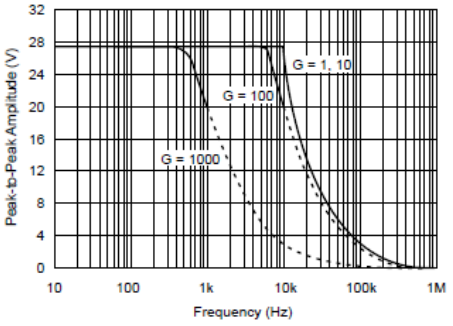

TYPICAL PERFORMANCE CURVES (CONT)

At T_A = +25°C, V_S = ±15V, unless otherwise noted.

SLEW RATE vs TEMPERATURE

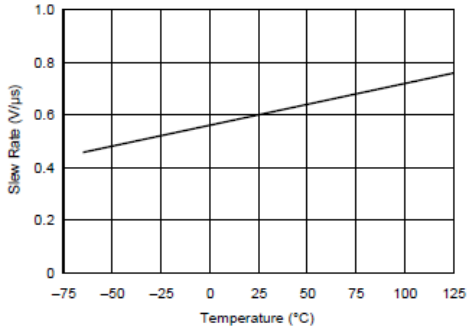

OUTPUT CURRENT LIMIT vs TEMPERATURE

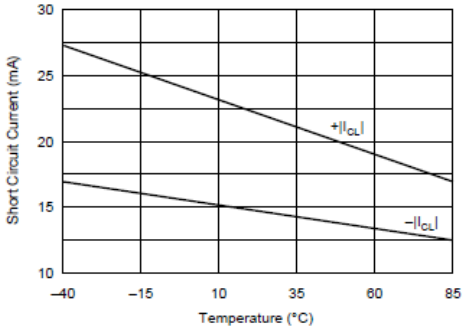

QUIESCENT CURRENT vs TEMPERATURE

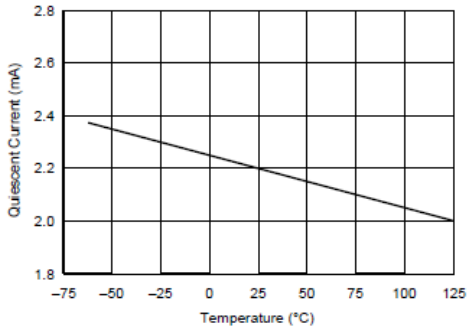

QUIESCENT CURRENT AND POWER DISSIPATION vs POWER SUPPLY VOLTAGE

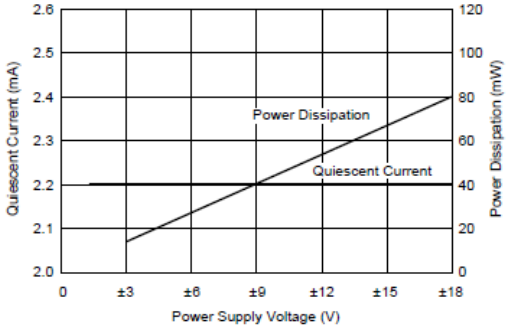

POSITIVE SIGNAL SWING vs TEMPERATUE (R_L = 2kΩ)

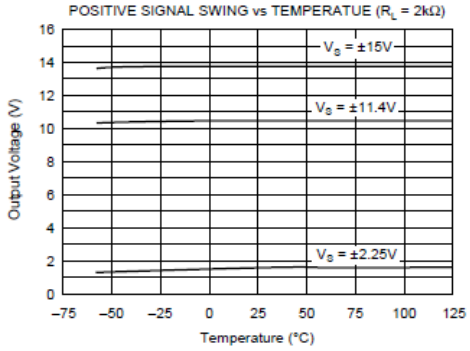

NEGATIVE SIGNAL SWING vs TEMPERATUE (R_L = 2kΩ)

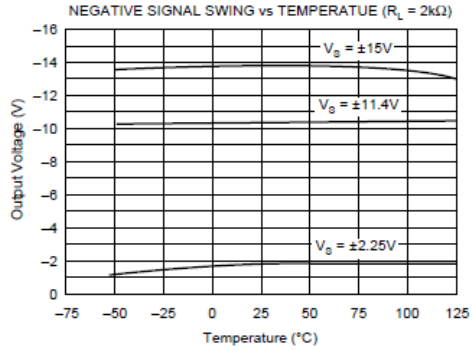

TYPICAL PERFORMANCE CURVES (CONT)

At T_A = +25°C, V_S = ±15V, unless otherwise noted.

LARGE SIGNAL RESPONSE, G = 1

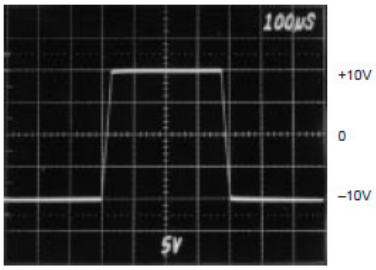

SMALL SIGNAL RESPONSE, G = 1

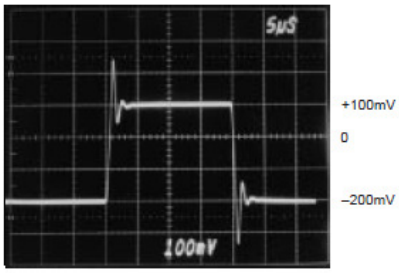

LARGE SIGNAL RESPONSE, G = 1000

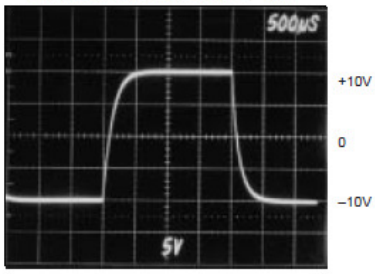

SMALL SIGNAL RESPONSE, G = 1000

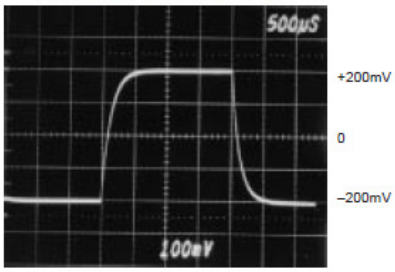

INPUT-REFERRED NOISE, 0.1 to 10Hz

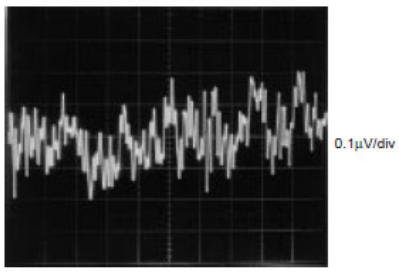

APPLICATION INFORMATION

Figure 1 shows the basic connections required for operation of the INA114. Applications with noisy or high impedance power supplies may require decoupling capacitors close to the device pins as shown.

The output is referred to the output reference (Ref) terminal which is normally grounded. This must be a low-impedance connection to assure good common-mode rejection. A resistance of 5Ω in series with the Ref pin will cause a typical device to degrade to approximately 80dB CMR (G = 1).

SETTING THE GAIN

Gain of the INA114 is set by connecting a single external resistor, R_G:

$$G = 1 + \frac{50\ k\Omega}{R_G} \qquad (1)$$

Commonly used gains and resistor values are shown in Figure 1.

The 50kΩ term in equation (1) comes from the sum of the two internal feedback resistors. These are on-chip metal film resistors which are laser trimmed to accurate absolute values. The accuracy and temperature coefficient of these resistors are included in the gain accuracy and drift specifications of the INA114.

The stability and temperature drift of the external gain setting resistor, R_G, also affects gain. R_G's contribution to gain accuracy and drift can be directly inferred from the gain equation (1). Low resistor values required for high gain can make wiring resistance important. Sockets add to the wiring resistance which will contribute additional gain error (possibly an unstable gain error) in gains of approximately 100 or greater.

NOISE PERFORMANCE

The INA114 provides very low noise in most applications. For differential source impedances less than 1kΩ, the INA103 may provide lower noise. For source impedances greater than 50kΩ, the INA111 FET-input instrumentation amplifier may provide lower noise.

Low frequency noise of the INA114 is approximately 0.4μVp-p measured from 0.1 to 10Hz. This is approximately one-tenth the noise of "low noise" chopper-stabilized amplifiers.

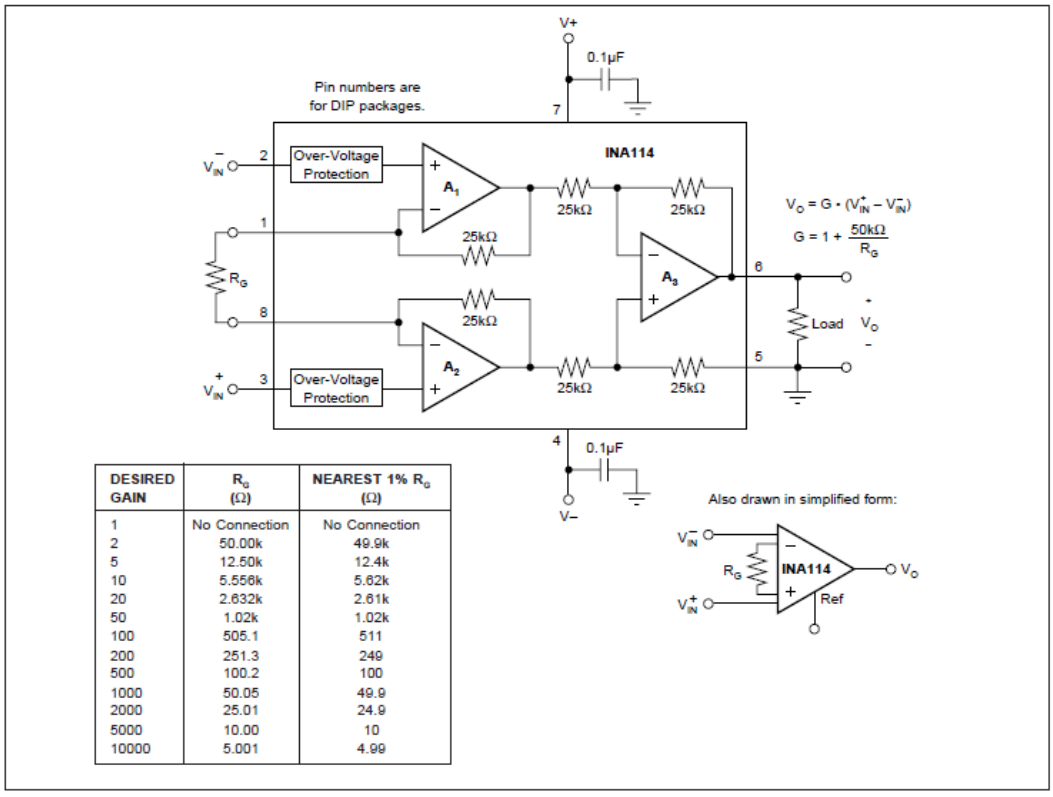

DESIRED GAIN	R_G (Ω)	NEAREST 1% R_G (Ω)
1	No Connection	No Connection
2	50.00k	49.9k
5	12.50k	12.4k
10	5.556k	5.62k
20	2.632k	2.61k
50	1.02k	1.02k
100	505.1	511
200	251.3	249
500	100.2	100
1000	50.05	49.9
2000	25.01	24.9
5000	10.00	10
10000	5.001	4.99

FIGURE 1. Basic Connections.

OFFSET TRIMMING

The INA114 is laser trimmed for very low offset voltage and drift. Most applications require no external offset adjustment. Figure 2 shows an optional circuit for trimming the output offset voltage. The voltage applied to Ref terminal is summed at the output. Low impedance must be maintained at this node to assure good common-mode rejection. This is achieved by buffering trim voltage with an op amp as shown.

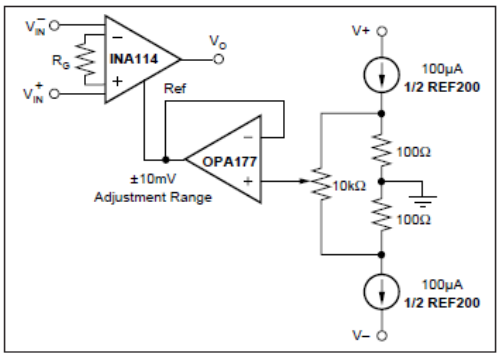

FIGURE 2. Optional Trimming of Output Offset Voltage.

INPUT BIAS CURRENT RETURN PATH

The input impedance of the INA114 is extremely high—approximately $10^{10}\Omega$. However, a path must be provided for the input bias current of both inputs. This input bias current is typically less than ±1nA (it can be either polarity due to cancellation circuitry). High input impedance means that this input bias current changes very little with varying input voltage.

Input circuitry must provide a path for this input bias current if the INA114 is to operate properly. Figure 3 shows various provisions for an input bias current path. Without a bias current return path, the inputs will float to a potential which exceeds the common-mode range of the INA114 and the input amplifiers will saturate. If the differential source resistance is low, bias current return path can be connected to one input (see thermocouple example in Figure 3). With higher source impedance, using two resistors provides a balanced input with possible advantages of lower input offset voltage due to bias current and better common-mode rejection.

INPUT COMMON-MODE RANGE

The linear common-mode range of the input op amps of the INA114 is approximately ±13.75V (or 1.25V from the power supplies). As the output voltage increases, however, the linear input range will be limited by the output voltage swing of the input amplifiers, A_1 and A_2. The common-mode range is related to the output voltage of the complete amplifier—see performance curve "Input Common-Mode Range vs Output Voltage."

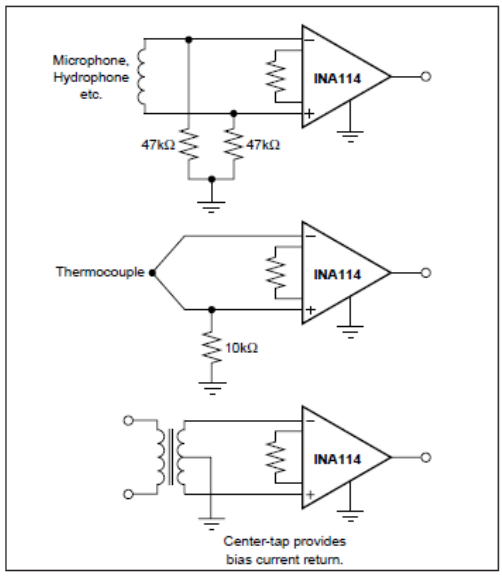

FIGURE 3. Providing an Input Common-Mode Current Path.

A combination of common-mode and differential input signals can cause the output of A_1 or A_2 to saturate. Figure 4 shows the output voltage swing of A_1 and A_2 expressed in terms of a common-mode and differential input voltages. Output swing capability of these internal amplifiers is the same as the output amplifier, A_3. For applications where input common-mode range must be maximized, limit the output voltage swing by connecting the INA114 in a lower gain (see performance curve "Input Common-Mode Voltage Range vs Output Voltage"). If necessary, add gain after the INA114 to increase the voltage swing.

Input-overload often produces an output voltage that appears normal. For example, an input voltage of +20V on one input and +40V on the other input will obviously exceed the linear common-mode range of both input amplifiers. Since both input amplifiers are saturated to nearly the same output voltage limit, the difference voltage measured by the output amplifier will be near zero. The output of the INA114 will be near 0V even though both inputs are overloaded.

INPUT PROTECTION

The inputs of the INA114 are individually protected for voltages up to ±40V. For example, a condition of –40V on one input and +40V on the other input will not cause damage. Internal circuitry on each input provides low series impedance under normal signal conditions. To provide equivalent protection, series input resistors would contribute excessive noise. If the input is overloaded, the protection circuitry limits the input current to a safe value (approximately 1.5mA). The typical performance curve "Input Bias Current vs Common-Mode Input Voltage" shows this input

current limit behavior. The inputs are protected even if no power supply voltage is present.

OUTPUT VOLTAGE SENSE (SOL-16 package only)

The surface-mount version of the INA114 has a separate output sense feedback connection (pin 12). Pin 12 must be connected to the output terminal (pin 11) for proper operation. (This connection is made internally on the DIP version of the INA114.)

The output sense connection can be used to sense the output voltage directly at the load for best accuracy. Figure 5 shows how to drive a load through series interconnection resistance. Remotely located feedback paths may cause instability. This can be generally be eliminated with a high frequency feedback path through C_1. Heavy loads or long lines can be driven by connecting a buffer inside the feedback path (Figure 6).

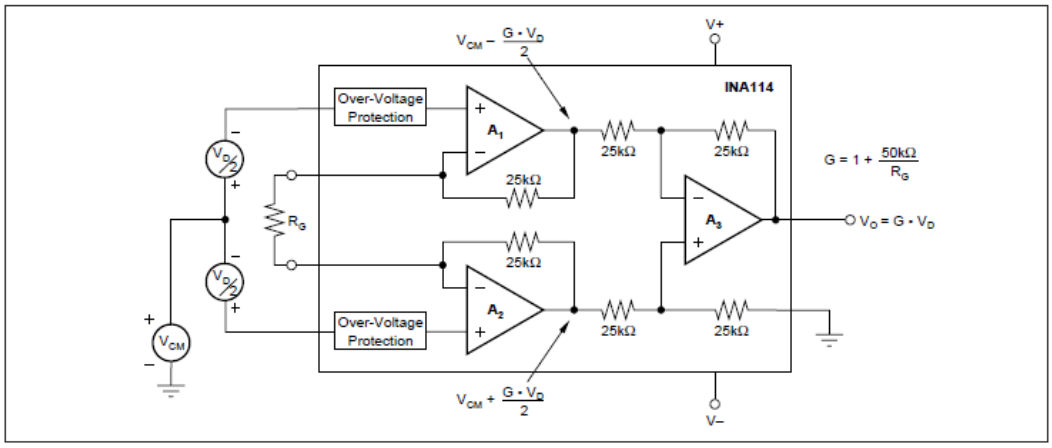

FIGURE 4. Voltage Swing of A_1 and A_2.

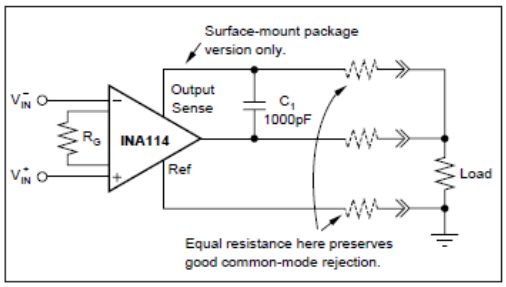

FIGURE 5. Remote Load and Ground Sensing.

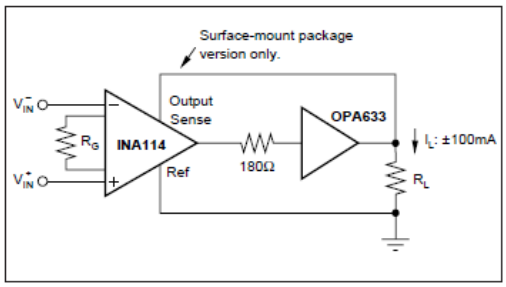

FIGURE 6. Buffered Output for Heavy Loads.

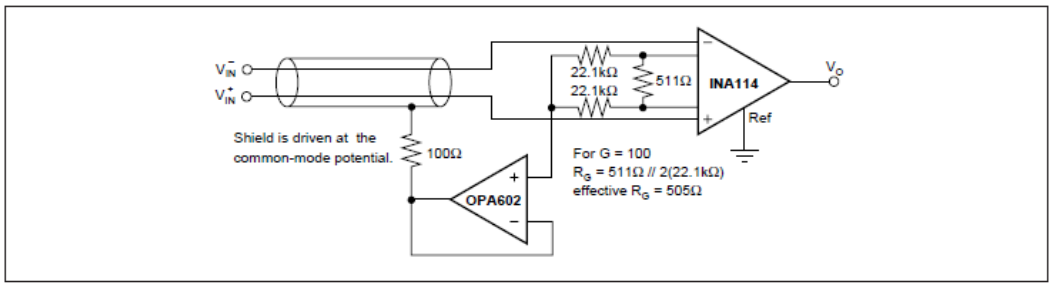

FIGURE 7. Shield Driver Circuit.

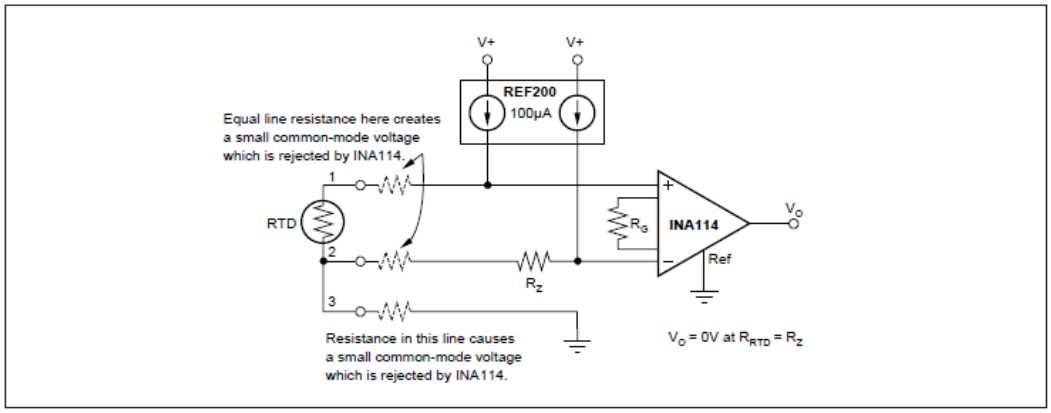

FIGURE 8. RTD Temperature Measurement Circuit.

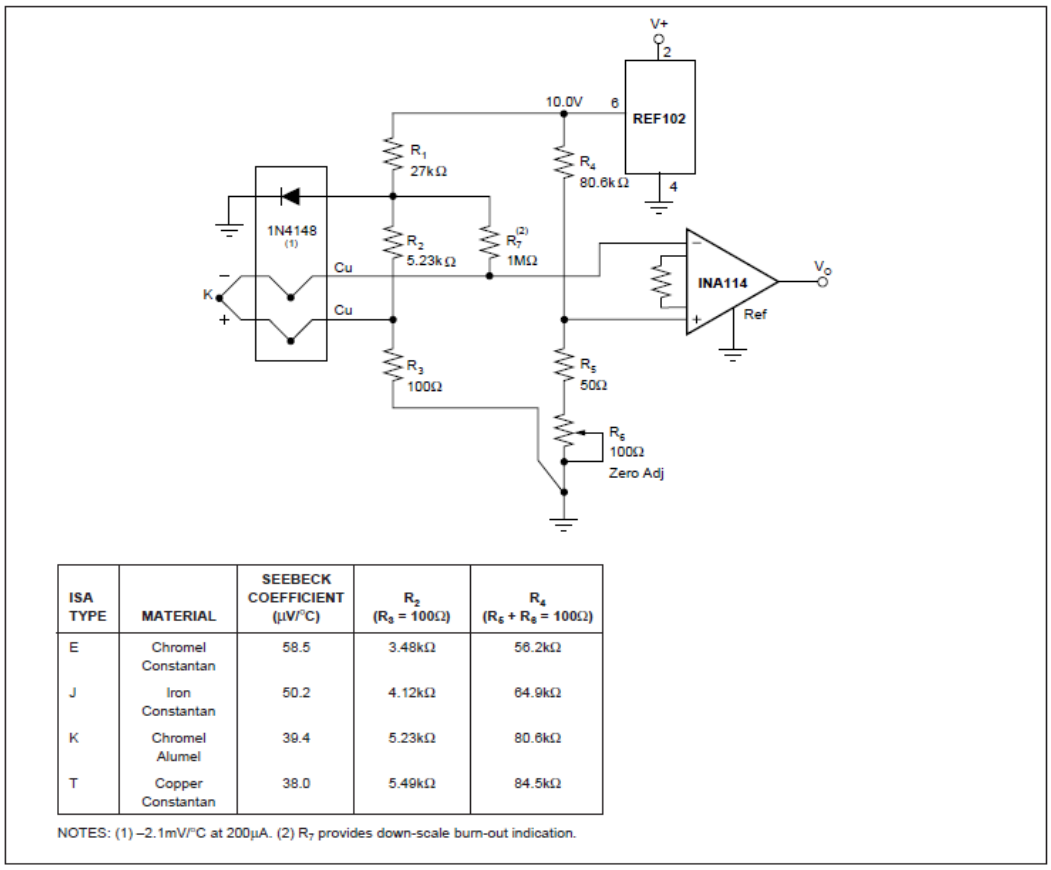

ISA TYPE	MATERIAL	SEEBECK COEFFICIENT (µV/°C)	R_2 (R_3 = 100Ω)	R_4 (R_5 + R_6 = 100Ω)
E	Chromel Constantan	58.5	3.48kΩ	56.2kΩ
J	Iron Constantan	50.2	4.12kΩ	64.9kΩ
K	Chromel Alumel	39.4	5.23kΩ	80.6kΩ
T	Copper Constantan	38.0	5.49kΩ	84.5kΩ

NOTES: (1) –2.1mV/°C at 200µA. (2) R_7 provides down-scale burn-out indication.

FIGURE 9. Thermocouple Amplifier With Cold Junction Compensation.

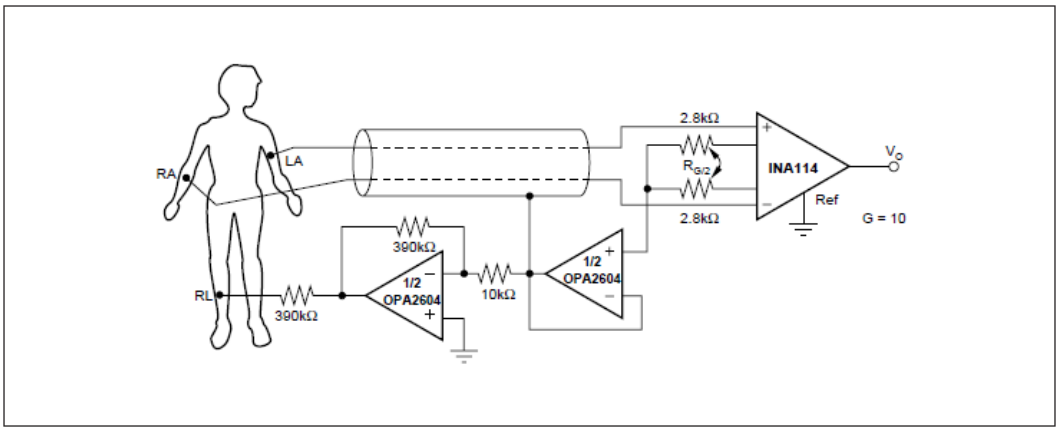

FIGURE 10. ECG Amplifier With Right-Leg Drive.

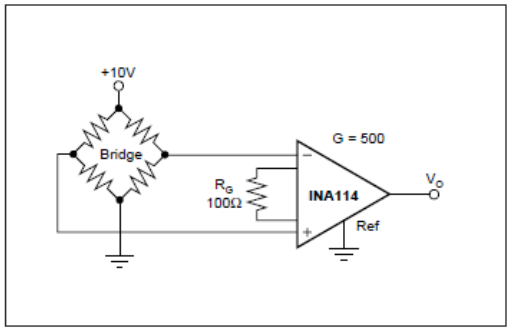

FIGURE 11. Bridge Transducer Amplifier.

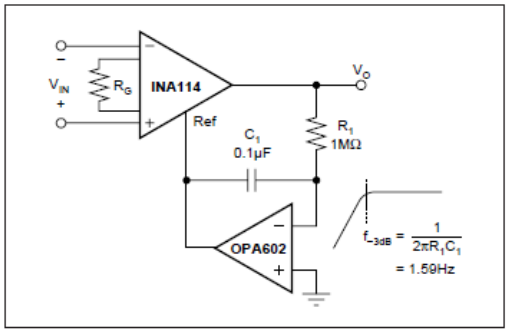

FIGURE 12. AC-Coupled Instrumentation Amplifier.

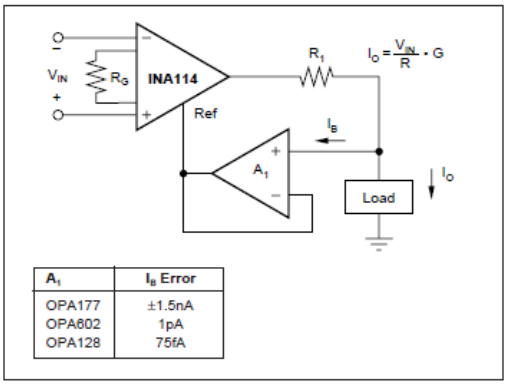

A_1	I_B Error
OPA177	±1.5nA
OPA602	1pA
OPA128	75fA

FIGURE 13. Differential Voltage-to-Current Converter.

IMPORTANT NOTICE

Texas Instruments and its subsidiaries (TI) reserve the right to make changes to their products or to discontinue any product or service without notice, and advise customers to obtain the latest version of relevant information to verify, before placing orders, that information being relied on is current and complete. All products are sold subject to the terms and conditions of sale supplied at the time of order acknowledgment, including those pertaining to warranty, patent infringement, and limitation of liability.

TI warrants performance of its semiconductor products to the specifications applicable at the time of sale in accordance with TI's standard warranty. Testing and other quality control techniques are utilized to the extent TI deems necessary to support this warranty. Specific testing of all parameters of each device is not necessarily performed, except those mandated by government requirements.

Customers are responsible for their applications using TI components.

In order to minimize risks associated with the customer's applications, adequate design and operating safeguards must be provided by the customer to minimize inherent or procedural hazards.

TI assumes no liability for applications assistance or customer product design. TI does not warrant or represent that any license, either express or implied, is granted under any patent right, copyright, mask work right, or other intellectual property right of TI covering or relating to any combination, machine, or process in which such semiconductor products or services might be or are used. TI's publication of information regarding any third party's products or services does not constitute TI's approval, warranty or endorsement thereof.